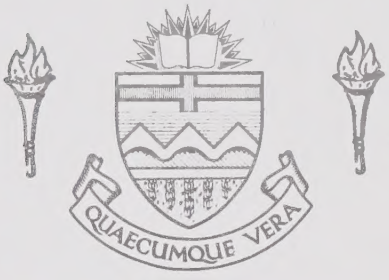

The University of Alberta
Printing Department
Edmonton, Alberta

THE UNIVERSITY OF ALBERTA

EXPERIMENTS ON STEEL WIDE-FLANGE BEAM-COLUMNS SUBJECTED TO LATERAL LOADS

by

© GORDON WAYNE ENGLISH

A THESIS

SUBMITTED TO THE FACULTY OF GRADUATE STUDIES

IN PARTIAL FULFILMENT OF THE REQUIREMENTS FOR THE DEGREE OF

MASTER OF SCIENCE

DEPARTMENT OF CIVIL ENGINEERING

EDMONTON, ALBERTA

SPRING, 1971

UNIVERSITY OF ALBERTA

FACULTY OF GRADUATE STUDIES

The undersigned certify that they have read, and recommend to the Faculty of Graduate Studies for acceptance, a thesis entitled EXPERIMENTS ON STEEL WIDE-FLANGE BEAM-COLUMNS SUBJECTED TO LATERAL LOADS submitted by GORDON WAYNE ENGLISH in partial fulfilment of the requirements for the degree of Master of Science.

ABSTRACT

This investigation was undertaken primarily to investigate experimentally the behavior of large scale beam-columns subjected to concentrated lateral loads. In addition, an attempt was made to correlate the maximum load carrying capacities of the beam-columns to those predicted by existing analytical procedures and thus provide the basis for a design method.

The results of tests on nine laterally loaded beam-columns of CSA G40.12 steel are reported herein. The restraint conditions, loading schemes and slenderness ratios of the members were varied to include a wide range of structural arrangements. All tests were continued until substantial unloading had occurred due to instability. The experimental results were predicted by a second-order elastic-plastic analysis.

The maximum load carrying capacities obtained from the test specimens were compared with those predicted by the modified interaction equations. The ratio of the load obtained experimentally to that predicted varied from 1.02 to 1.13 with a mean value of 1.09 for the nine specimens. Thus the modified interaction equations are conservative, yet predict the ultimate capacities with a reasonable degree of accuracy. Since the specimens were designed to include a wide range of structural parameters, the modified interaction equations provide a rational method for designing laterally loaded beam-columns.

ACKNOWLEDGEMENTS

This study forms a part of a continuing investigation into the behavior of steel members and frames, in progress at the Department of Civil Engineering, University of Alberta. P.F. Adams is the Project Director. The project receives financial support from the Canadian Steel Industries Construction Council, the National Research Council of Canada and the Defence Research Board.

The author wishes to acknowledge the continuing encouragement and assistance of P.F. Adams who supervised the work leading to the dissertation. The comments and constructive criticisms of J.S. Kennedy and J. Longworth, who served on the thesis committee are gratefully acknowledged.

The assistance of H. Panse and members of the laboratory staff in the performance of the testing program, D.J.R. Delicate in the presentation of the data and Mrs. B. Gallaiford, who typed the thesis, is also acknowledged.

TABLE OF CONTENTS

LIST OF TABLES

LIST OF FIGURES

CHAPTER I

INTRODUCTION

In a framed structure an individual member may be subjected to an axial force or to bending moments acting alone or in combination. Where a member is subjected to forces producing significant amounts of both bending and compression, it is classified as a beam-column (19).

In such a member the ultimate strength will be reached when the bending moment, at a point of support, is equal to the reduced (for axial load) plastic moment capacity, or when the entire member is subjected to forces and bending moments producing inelastic instability. For a beam-column, the elastic limit is not indicative of the ultimate strength and for this reason beam-columns in building structures are designed using empirical relationships which do provide an index of the ultimate strength (9).

The beam-column, shown schematically in FIG. 1.1(a), is typical of members in building structures where moments are applied at the member ends. The member is of length, L, and is subjected to a constant axial load, P, and equal end moments, M_o, which increase monotonically to deform the column in a symetrical single curvature mode. The deformation is characterized by the end rotation, θ. The member is assumed to be pinned at both ends and translation is prevented.

The bending moment at any point is equal to the sum of the primary bending moment caused by the applied end moments and secondary moments produced by the axial force acting through the deflection, Δ. FIG. 1.1(b), shows schematically the two contributions as well as the total bending moment distribution along the column length. Because the bending moment distribution on the column depends on the deflected shape, the ultimate strength can not be obtained directly. Instead, a series of points defining the moment-rotation (M_o-θ) curve for the member must be established by a numerical process, which takes into account the gradual yielding of the cross-section due to the applied forces and the residual strain distribution (10). The peak of this curve represents the maximum value of M_o that can be maintained under the prescribed axial force, P. The M_o-θ curve, and thus the ultimate strength, depends on the ratio of P/P_y, where P_y is the yield load, and L/r_x, where r_x is the strong axis radius of gyration, for rolled wide flange shapes. A typical M_o-θ curve is shown in FIG. 1.2.

The same approach has been used to establish M_o-θ curves for columns subjected to a single end moment, to equal and opposite end moments, and a variety of other conditions (16).

The above procedure is time consuming and not easily adaptable to the design situation. To facilitate the design of beam-columns, the ultimate strength has been estimated by using "interaction equations" (7). These equations relate the applied end moments and axial force to limiting values of the same quantities. The equations

account for slenderness effects, boundary conditions and variations in the bending moment along the member length. Although the interaction equations are empirical they predict the ultimate strength of a beam-column with a reasonable degree of reliability and have become accepted as a convenient tool in the design of beam-columns in ordinary frames.

Beam-columns subjected to lateral loads (or lateral loads combined with bending moments) applied at locations between points of support, occur frequently in industrial structures. FIG. 1.3 shows schematically a beam-column subjected to a concentrated lateral load, R.

In the present specifications, two approaches are suggested for applying the interaction equations to laterally loaded columns. The first is basically an extension of the elastic limit solution to a few particular cases of loading (8). The second treats the laterally loaded column as an assemblage of two column segments, each subjected to end moments (7). This second approach permits the designer to treat a much wider range of loading and support conditions.

Before either approach can be used with confidence, however, experimental evidence concerning the behavior of laterally loaded beam-columns is required. The primary object of this report is to describe the result of a testing program performed on specimens consisting of a laterally loaded column restrained by girders framing into either end. The restraint conditions, loading scheme and slenderness ratios of the members were varied to include a wide range of structural arrangements.

Summaries of previous investigations of laterally loaded beam-columns are presented in CHAPTER II. In CHAPTER III, the experimental program is described and the test procedure is discussed in detail. The results obtained from the test program are presented in CHAPTER IV and a discussion of these results is included in CHAPTER V. Finally, the report is summarized in CHAPTER VI.

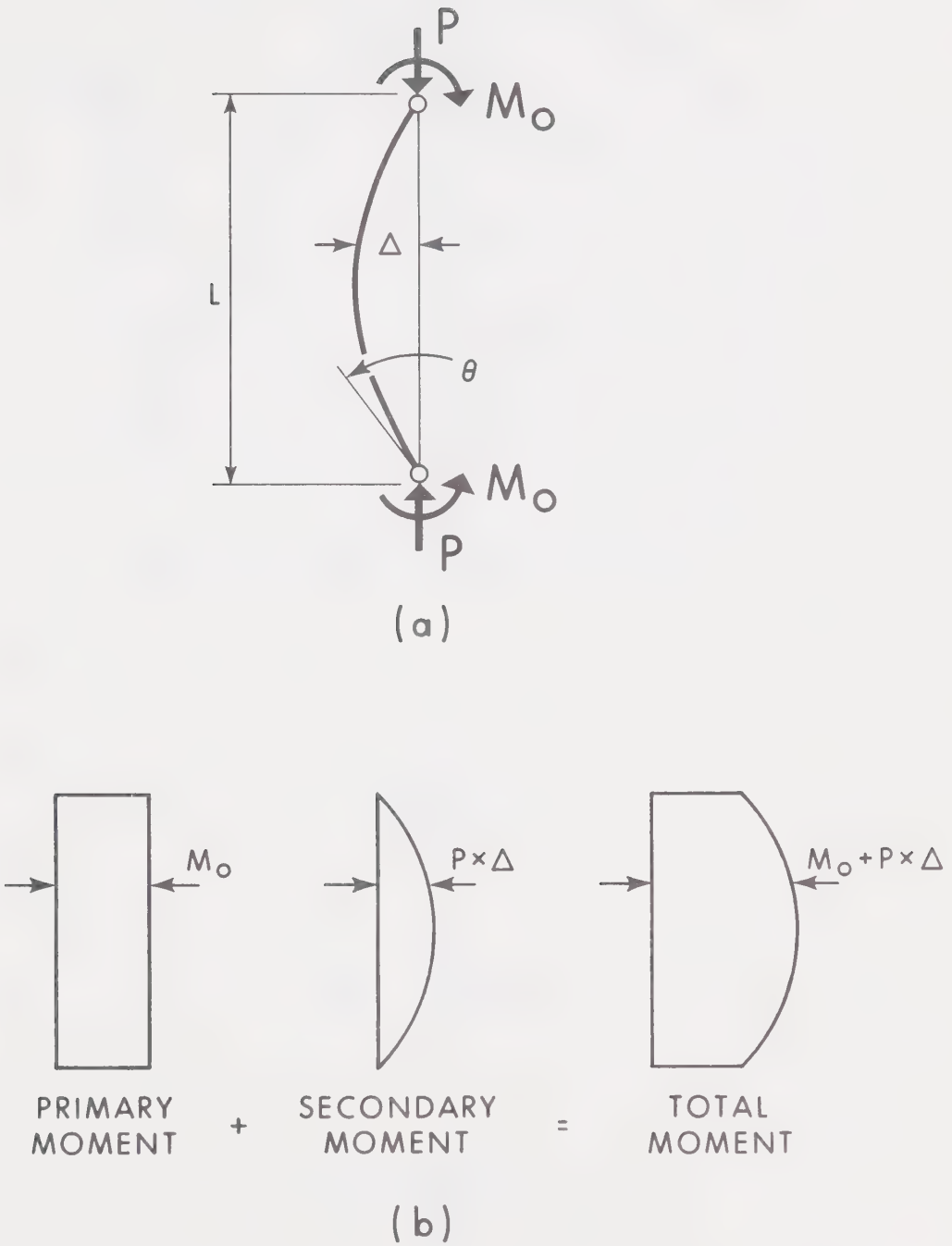

FIG. 1.1 COLUMN SUBJECTED TO EQUAL END MOMENTS

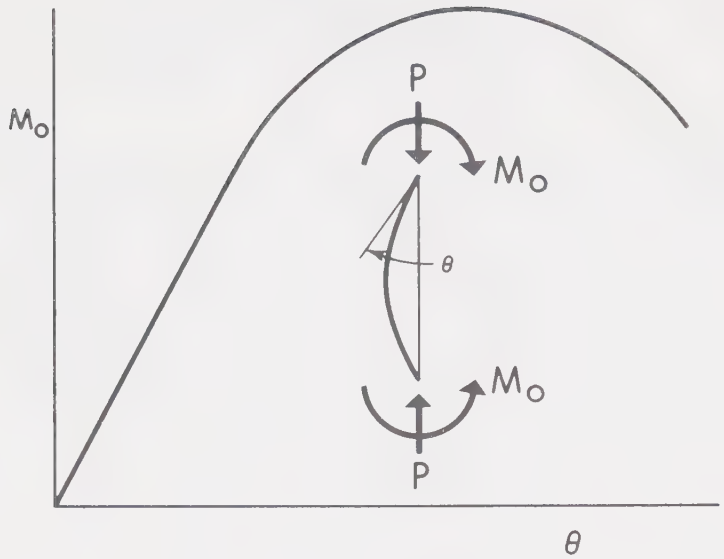

FIG. 1.2 MOMENT-ROTATION RELATIONSHIP

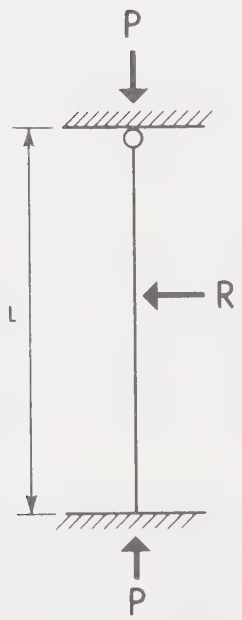

FIG. 1.3 LATERALLY LOADED COLUMN

CHAPTER II

PREVIOUS INVESTIGATIONS

Introduction

Most beam-columns in building structures are subjected to axial forces and to moments applied at the member ends, thus, this loading case has been the subject of extensive research (10, 19). Analytical procedures have been developed to predict the behavior of such members. These procedures account for the effects of inelastic action, produced by the initial residual strain distribution acting in combination with strains produced by the applied loads. In addition, the predicted results have been verified by comparison with the results of extensive testing programs on large scale specimens (14). From these investigations, a design procedure based on the empirical interaction equations, has been developed for the design of beam-columns subjected to end moments (9). The design procedure is outlined in APPENDIX A.

In contrast, only a few scattered investigations have attempted to study the behavior of beam-columns subjected to transverse loads. In particular, experimental work in this area is almost non-existent.

Analysis and Design of Laterally Loaded Beam-Columns

For a beam-column subjected to transverse loads, the deflected shape may be obtained as the solution to the differential equation expressing the equilibrium of the member in the deformed condition (20). The solution reflects the loading condition as well as

the boundary conditions at the member ends. For all cases, the maximum deflection, Δ, can be expressed as the product of the deflection, $\bar{\Delta}$, from a first order elastic analysis, times an amplification factor. Similarly, the maximum moment, M, can be expressed as the product the moment, $\bar{M}$, from a first order elastic analysis, times a second amplification factor. The amplification factors are functions of the applied axial force and reflect the stiffness of the member and its boundary conditions. In cases for which the deflected shape can be reasonably approximated by a sine wave, the amplification factors are both given by $1/ (1 - P/P_e)$ where P denotes the axial force on the member and P_e is the Euler load. For many other cases the deflection amplication factor can again be approximated by the above expression. In these cases, however, the maximum bending moment, M, is more closely approximated by :

$$M = \bar{M} + P \Delta \tag{2.1}$$

or

$$M = \bar{M} + P \bar{\Delta} \frac{1}{1 - P/P_e} \tag{2.2}$$

Eqn. 2.2 may be rearranged as :

$$M = \bar{M} \frac{1 + \psi P/P_e}{1 - P/P_e} \tag{2.3}$$

where

$$\psi = \frac{\pi^2 \bar{\Delta} E I}{\bar{M} L^2} - 1 \tag{2.4}$$

In Eqn. 2.4, E denotes the modulus of elasticity of the material and I is the moment of inertia of the member. The value of ψ has been determined for several simple cases of transverse loading, for example, for a pin-ended column subected to a concentrated load, R, at mid-height:

$$\bar{M} = \frac{R\ L}{4} \qquad (2.5\ a)$$

$$\bar{\Delta} = \frac{R\ L^3}{48\ E\ I} \qquad (2.5\ b)$$

$$P_e = \frac{\pi^2\ E\ I}{L^2} \qquad (2.5\ c)$$

therefore $\psi = -0.178\ P/P_e$ (2.6)

and $M = \bar{M}\ \frac{1 - 0.178\ P/P_e}{1 - P/P_e}$ (2.7)

Similar expressions have been tabulated for other loading and boundary conditions (9).

An elastic solution, however, does not provide a reliable indication of the load carrying capacity of a beam-column. The ultimate strength has been accepted as the basis for the design of such members by both the allowable stress method and the plastic strength technique (9).

To determine the ultimate strength, Ketter and Galambos have presented a numerical procedure for beam-columns subjected to end moments (10). For given values of the axial load, cross-section and member length, the procedure predicts the end moment-rotation relationship for the beam-column. The basic building block used in this technique is the moment-thrust-curvature (M-P-ϕ) relationship for the cross-section as shown in FIG. 2.1(a). The member is sub-divided into segments and an initial value of the end moment selected. Deflection values are assumed at each node point along the member length and moments computed as shown in FIG. 2.1(b). From the

M-P-ϕ relationship, the corresponding curvatures are established and new deflections computed. If the computed deflections do not correspond to those assumed, the procedure is repeated using the computed set of deflections as a starting point. Thus one point on the moment-rotation relationship is established. By repeating this procedure for various end moments, the complete relationship can be determined. The ultimate moment (for that particular length and assumed axial thrust) corresponds to the peak of the moment-rotation relationship. This procedure was repeated for various assumed axial thrusts, member lengths and end moment ratios. Plots of the axial load, P, non-dimensionalized by P_y, the yield load, versus the end moment, M_o, non-dimensionalized by M_p, the plastic moment capacity, are shown in FIG. 2.1 (c). The curves shown in FIG. 2.1 (c) are for a member subjected to a single end moment and having selected values of the slenderness ratio, L/r_x. In a subsequent study, Ketter superimposed the solutions for two members subjected to single end moments and thus obtained the ultimate strength for pin-ended columns subjected to concentrated loads at mid-height (11).

Lu and Kamalvand used a numerical integration procedure to determine the ultimate strength of laterally loaded beam-columns subjected to four different conditions (17). The four cases are shown in FIG. 2.2 (a) and included both pin-ended and fixed-ended columns subjected to either a uniformly distributed load or a concentrated load applied at the mid-point of the member. Ultimate

strength interaction curves were obtained for the four cases. FIG. 2.2 (b) shows the curve for pin-ended columns subjected to central concentrated loads.

Lu and Kamalvand suggested that an equivalent moment factor (which was numerically equivalent to the $1 + \psi\ P/P_e$ term from the elastic limit theory) could be used to determine the ultimate strength of a beam-column from a modified version of the interaction equations. In order to check this assumption the ultimate strengths of the members were computed by the analytical procedure and compared with the strengths predicted by the interaction equations using an equivalent moment factor, C_m, obtained from the elastic solution. FIG. 2.3 shows the results obtained for the pin-ended and fixed-ended cases subjected to concentrated, mid-point loads. The open circles represent the analyical solution and the straight line represents the interaction equation. In these figures, $C_m = 1 - 0.2\ P/P_e$ for the pin-ended case and $C_m = 1 - 0.6\ P/P_e$ for the fixed-ended column. Similar results were obtained for the uniformly loaded members. Since the modified interaction equations predicted the ultimate strength of the members conservatively, these equations are used for the design of laterally loaded beam-columns subjected to the particular conditions of the study (17).

Lay had previously suggested an analyical procedure for determining the load-deflection relationship for a beam-column subjected to a concentrated lateral load by using the M-θ curves

for columns subjected to end moments (12). For a given column and given axial thrust the load-deformation relationship of the member is obtained by dividing the column into two segments at the point of load application, as shown in FIGS. 2.4 (a) and (b). For a particular value of the load-point deflection, the moment at the load-point is assumed. Then, from the appropriate M-θ curve for each segment, the end rotations are found as shown in FIG. 2.4 (c). Finally the continuity condition at the load-point is checked. If the initial choice of the bending moment is correct, the rotations will be compatible and the end shears of the two segments are computed. In this manner one point on the load-deflection relationship is obtained. The procedure is repeated until the complete load-deflection relationship, as shown in FIG. 2.4 (d), is obtained.

Adams used the same segmental approach to analyze laterally loaded beam-columns subjected to concentrated loads with either pin-ended or fixed-ended boundary conditions (2). Adams and McLellan have also shown that the segmental approach can be used to analyze members subjected to other intermediate loading (moment and axial load) conditions (4, 3).

Adams proposed that that the segmental approach could be extended to the design of laterally loaded beam-columns subjected to concentrated loads (2). Each segment is treated as a column subjected to end-moments and free to sway. Therefore, when applying the interaction equations, a C_m factor of 0.85 (in conjunction with the maximum end moment on the segment) should be used (24).

In order to verify this procedure, the ultimate strength of a number of symmetrical pin-ended and fixed-ended columns were computed and compared to the ultimate strengths predicted by the interaction equations, using $C_m = 0.85$. The results are shown in FIG. 2.3. The solid circles now represent the analytical solutions and the straight line again represents the interaction equation, with $C_m = 0.85$. The ultimate strengths predicted using this form of the interaction equations closely approximate the analytical results. The segmental design approach can easily be extended to columns subjected to non-symmetrical lateral loading conditions, to other intermediate loading conditions and non-symmetrical boundary conditions (4).

Previous Experimental Investigations

Previous experimental investigations of laterally loaded beam-columns are limited in number and in scope. Paris reported the results of tests on small scale members subjected to two symmetrical concentrated loads. However the tests were restricted to the elastic range (18). Wright reported the results of tests on small scale rectangular and wide flange members subjected to various loading and restraint conditions (21, 22). The specimens were deformed well into the inelastic range. The details and major results of these tests are outlined in APPENDIX B.

In recent years experimental investigations have attempted to consider the action of portions of the total structure, instead of isolated members. For example, a testing arrangement which has been used to test frames containing critically loaded beam-columns

is outlined in APPENDIX C. A subassemblage, consisting of a beam-column and two restraining beams is used to simulate the action of a portion of the actual structure. A similar test arrangement would appear to be applicable to the experimental investigation of laterally loaded beam-columns.

Summary

In contrast to the extensive investigation into the behavior of beam-columns subjected to end moments, relatively little work has been performed on laterally loaded beam-columns. Methods are available to predict the load-deflection relationship for such members, however, and design procedures have been proposed which can be applied to members having a variety of loading and boundary conditions. Experimental work relating to laterally loaded columns is almost non-existent and those investigations which have been reported have utilized small scale specimens. It is the purpose of this investigation to perform a series of large scale tests on laterally loaded beam-columns. The test specimens will consist of beam-columns and adjacent restraining beams. The results of the tests will be used to verify the analytical procedures and will form the basis for design methods.

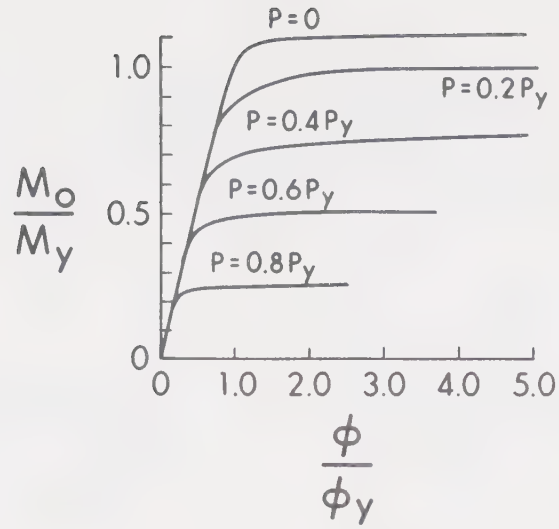

(a) M-P-ϕ RELATIONSHIP

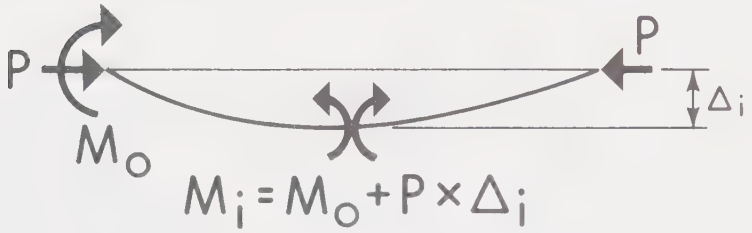

(b) DEFLECTED SHAPE

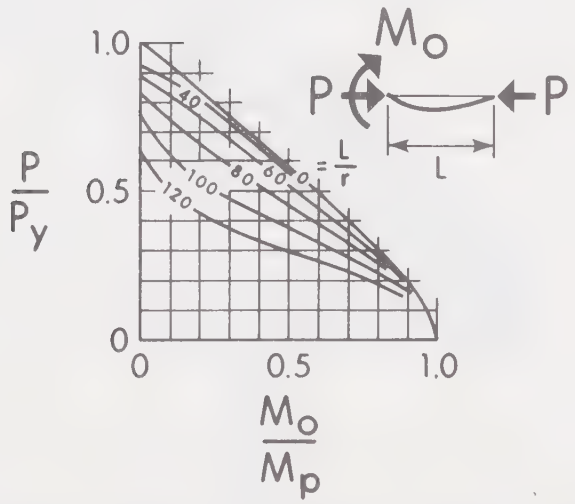

(c) ULTIMATE STRENGTH INTERACTION CURVES

FIG. 2.1 COLUMN SUBJECTED TO SINGLE END MOMENT

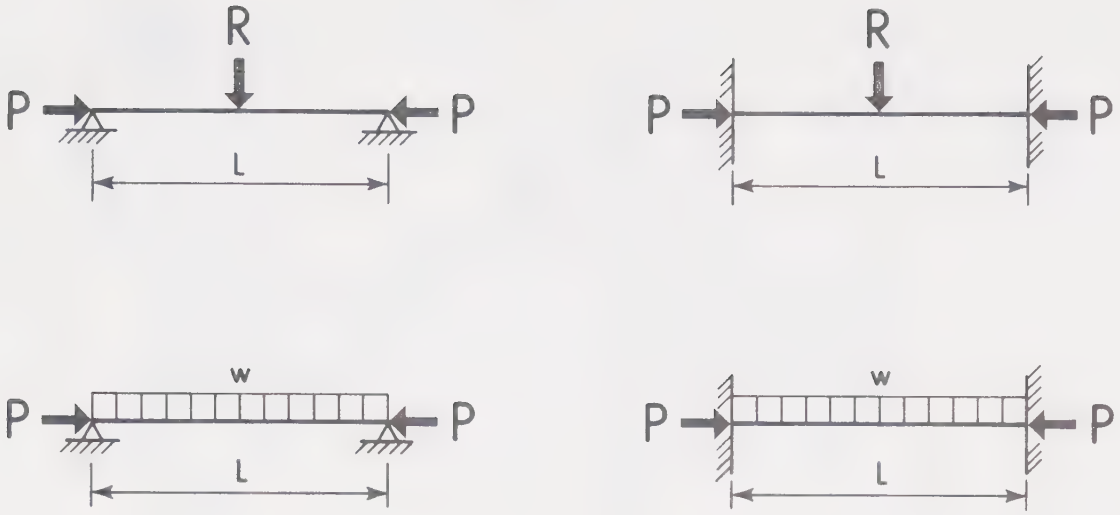

(a) LOADING CONDITIONS

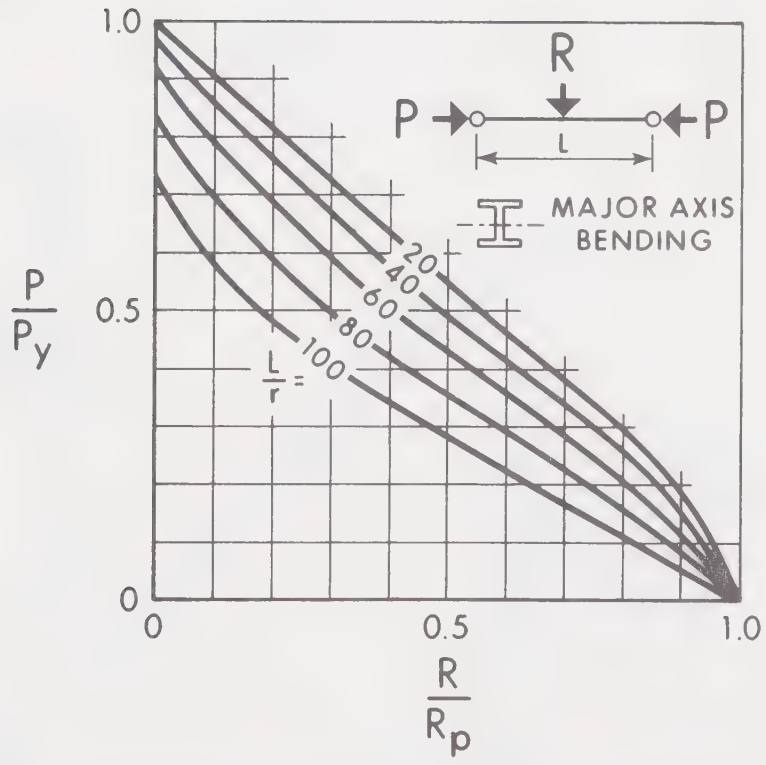

(b) ULTIMATE STRENGTH INTERACTION CURVES

FIG. 2.2 LATERALLY LOADED BEAM-COLUMN

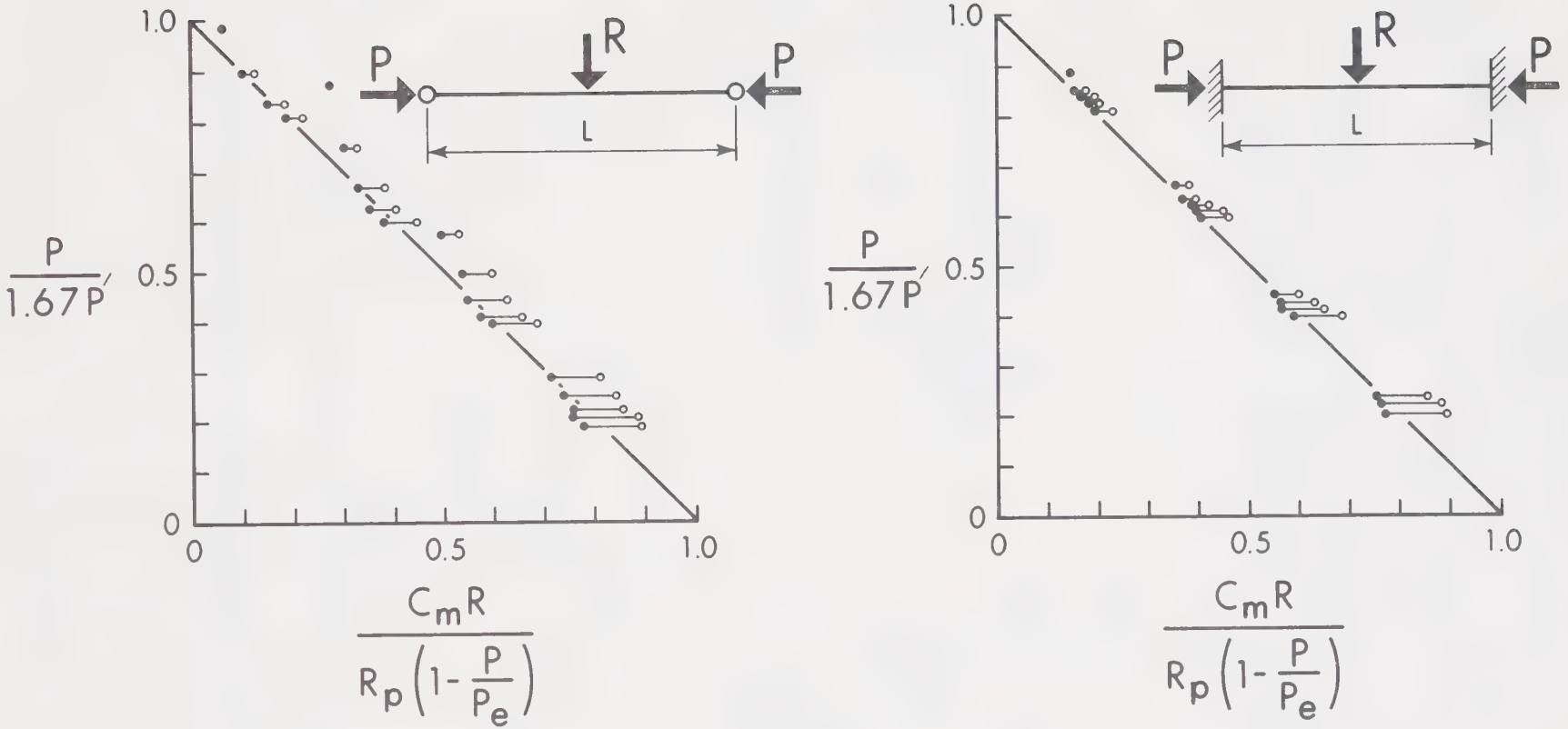

FIG. 2.3 MODIFIED INTERACTION EQUATIONS

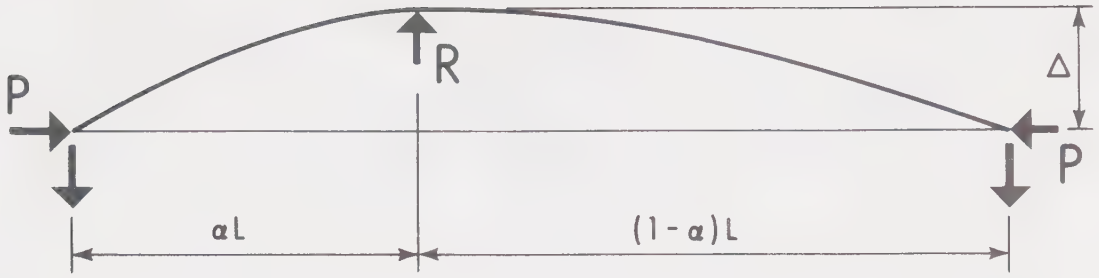

(a) LATERALLY LOADED COLUMN

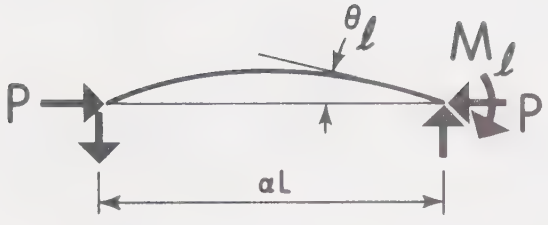

(b) LEFT SEGMENT

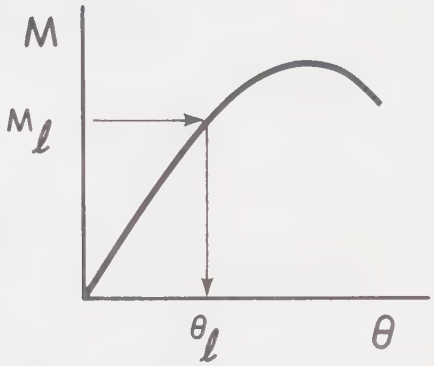

(c) SEGMENT M-θ RELATIONSHIP

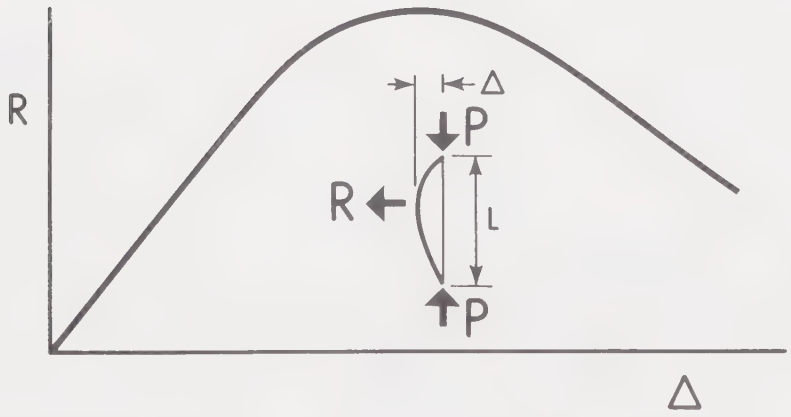

(d) LOAD-DEFLECTION RELATIONSHIP

FIG. 2.4 SEGMENTAL ANALYSIS

CHAPTER III

EXPERIMENTAL PROGRAM

Scope

The experimental program consisted of a series of nine tests on subassemblages fabricated from rolled wide-flange members of CSA G40.12 steel (6). The lengths used for the test series had been cold-straightened by rotarizing and all lengths were rolled from the same heat.

Eight of the specimens consisted of a single beam-column and restraining beams at either end; one test was performed on a beam-column without restraints. The lateral loads were applied to the members at either the mid-point or the upper third-point. The testing arrangement is shown schematically in the inset to TABLE 3.1. A typical moment distribution is also shown in this inset.

Specimen Details

All columns and beams were fabricated from W5x16 (5 WF 16) sections. The restraint and loading condition, as well as the slenderness of the column, was varied throughout the series. In TABLE 3.1 the specimen dimensions are listed; L_{g1} denotes the length of the upper beam, L_{g2} the length of the lower beam and L_c is the length of the column. Also indicated in this table is the point of lateral load application (mid-height or upper third-point).

The specimens were fabricated using standard techniques,

however, special details were used to transfer the axial load into the members and to provide for reactions at the ends of the restraining beams. At the rigidly connected beam-to-column joints, doubler plates were welded to the flange tips to provide additional shear capacity and to provide support for a two inch diameter shaft, which was attached to the web at the geometric center of the connection. (The ends of the shaft fitted into lugs, provided with bearings, and the lugs were used to transfer the axial load into the column.) A similar arrangement was used (to provide pinned reactions) at the far end of the restraining girders, except that in these cases the pin was loose fitting to provide for adjustment. Web stiffeners were attached to the members at various points to receive lateral braces (lateral braces were used to prevent premature out-of-plane deflections).

Material and Section Properties

The chemical composition for the steel used in the program is given in TABLE 3.2 along with the mill test results. These conform to the CSA G40.12 specification (6).

TABLES 3.3 and 3.4 summarize the material properties obtained from laboratory tension tests performed on specimens cut from two different lengths of the member. The locations on the cross-section, from which the coupons were taken are shown in the insets. In TABLE 3.3 and 3.4, σ_y denotes the static yield stress, σ_u denotes the

ultimate stress, ε_y is the calculated yield strain corresponding to a modulus of elasticity, E=29,600 ksi, ε_{st} is the measured strain at the onset of strain-hardening and E_{st} is the strain-hardening modulus (1). The residual stress distribution over the cross-section is shown in the inset to TABLE 3.4. This distribution is typical of that for rotarized beams.

A summary of the measured cross-sectional dimensions is given in TABLE 3.5. The depth, d, flange width, b, flange thickness, t, and web thickness, w, were determined by measuring the specimens used in the test program. The cross-sectional area, A, radius of gyration about the strong axis, r_x, the moment of inertia, I, and the plastic section modulus, Z, were calculated from the measured dimensions; these are also listed in TABLE 3.5. (The in-plane moment of inertia and plastic section modulus for the upper beam used in BC-9 are also specified.)

In the prediction of the specimen behavior, measured values of material properties and cross-sectional dimensions were used throughout.

Test Set-Up

A cut-away diagram of the test set-up is shown in FIG. 3.1. The jacks used to apply both vertical and lateral loading are shown along with the reaction arrangements. FIG. 3.2 shows an overall view of the test set-up. The test specimen or subassemblage appears in white in the photograph.

The vertical beam-column member, shown in FIG. 3.2, was loaded in compression by hydraulic jacks at its lower end. The jacks reacted against the laboratory floor. The reaction from the column was transferred through a spreader beam to the auxiliary frame, which in turn was bolted to the laboratory floor (FIG. 3.1). The lateral load was applied by a tension jack, at the mid-height of the column as shown in FIG. 3.2. The reaction from the jack was taken by cross-beams into the auxiliary frame. As the specimen was loaded, the beam-to-column joints rotated, developing moments and shears in the restraining beams. The reactions from the lower beam was transferred directly into the laboratory floor; that from the upper beam was taken into the spreader beam and then into the auxiliary frame.

The vertical load was applied by hydraulic jacks acting in compression. The hydraulic pressure was provided by an Amsler Pendulum Dynamometer and the jack arrangement was pre-calibrated so that the vertical load could be computed directly from the pressure reading. These jacks reacted against the laboratory floor as shown in FIG. 3.3 (a) and transferred the axial load to the column through a lug-bearing-shaft arrangement at the bottom column end as shown in FIG. 3.3 (b). Bearings were incorporated between the lug and shaft to minimize the effect of friction. A similar lug-bearing-shaft arrangement was employed at the column top to transfer the vertical load reaction to the spreader beam.

The lateral load was applied by a hydraulic jack acting in tension. The hydraulic pressure was supplied by an air over oil pump (23). A load cell was incorporated into the shaft of the jack, to provide a measure of the lateral load. This load was applied to the column through a box bolted to the web stiffener. The box was constructed to contact the specimen only at the stiffener and to provide ample clearance for buckling of the compression flange. This jacking arrangement reacted against the auxiliary frame. FIG. 3.4 shows the lateral load arrangement.

The restraining beam reactions incorporated a lug-bearing-shaft arrangement, similar to that employed for vertical load application, as shown in FIG. 3.5. Prior to testing, the ends of both beams were jacked upwards to relieve the subassemblage of beam dead load moments and the end of the lower beam was jacked up an additonal amount equal to the anticipated axial shortening of the column; at this stage the reaction pins were inserted in the bearings.

Lateral bracing of the beams was provided by steel rods bolted in a horizontal position between the auxiliary frame and stiffeners attached to the specimen, as shown in FIG. 3.6. The braces on the beam-column, however, were articulated, which prevented out-of-plane movement at the braced point while allowing the specimen to deform in its own plane (23). The articulated braces reacted against the auxiliary frame. This bracing system is shown in FIG. 3.7.

The test specimens were instrumented so that the bending moments and forces could be determined at points of interest in each member segment. The strain gages were placed at locations which remained elastic throughout the test. Each of the restraining beams was gaged in two locations as shown in FIG. 3.8. The inset to FIG. 3.8 shows the placement of the gages on the beam cross-section. Each column was gaged in two locations below and two locations above the load point as shown in FIG. 3.8. The placement of the gages on the column cross-section is shown on the inset to FIG. 3.8. The deflections of the columns were measured at the load-point by a transducer and a dial gage and at each of the column gage locations by a transducer. In addition, a transducer was placed at each end of the column to detect any rigid body movements.

Additional instrumentation consisted of six rotation meters, two on the restraining beams and four on the column, as shown in FIG. 3.8 and a dial gage to measure the column axial shortening.

Each specimen was white washed before testing to aid in observing the progression of yielding.

Test Procedure

Each specimen was first subjected to full vertical load. The load was maintained at a constant value throughout the test.

Initially the specimen was deformed by increasing the hydraulic pressure in the lateral loading jack to predetermined values. The load was maintained at each of these values until all readings had been taken.

After yielding had occurred in the specimen, the test progressed by increasing the flow of fluid to the ram in order to increase the load-point deflection; at preselected stages the flow of hydraulic fluid was closed off for a five minute period before readings were taken. In addition to the instrument readings mentioned in the previous section, visual observations of the progression of yielding and buckling were recorded for each increment. The specimens were deformed well into the unloading range using the above procedure.

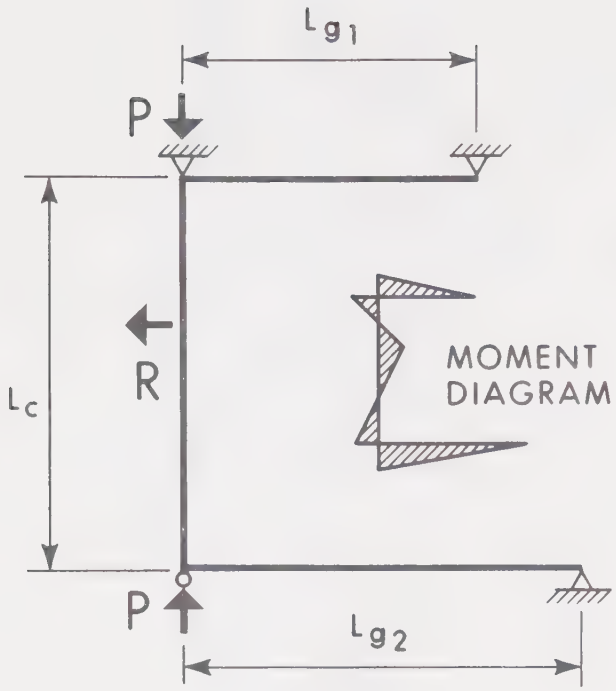

Test	Point of Load Application	L_c (in)	L_{g1} (in)	L_{g2} (in)
BC-1*	Mid-height	170	--	--
BC-2	Mid-height	240	120	168
BC-3	Mid-height	240	120	168
BC-4	Mid-height	170	120	168
BC-5	Mid-height	170	120	168
BC-6	Upper third-point	240	120	168
BC-7	Upper third-point	240	120	168
BC-8	Upper third-point	170	120	168
BC-9**	Upper third-point	170	60	120

Note: * Tested without restraining beams.

** Upper beam bent about weak axis.

TABLE 3.1 SPECIMEN DIMENSIONS

CHEMICAL COMPOSITION %					MILL TEST RESULTS		
C X100	Si X100	Mn X100	P X1000	S X1000	YIELD STRESS (ksi)	ULTIMATE STRESS (ksi)	ELONGATION %
22	27	118	15	14	59.3	88.2	24

TABLE 3.2 CHEMICAL COMPOSITION AND MILL TEST RESULTS

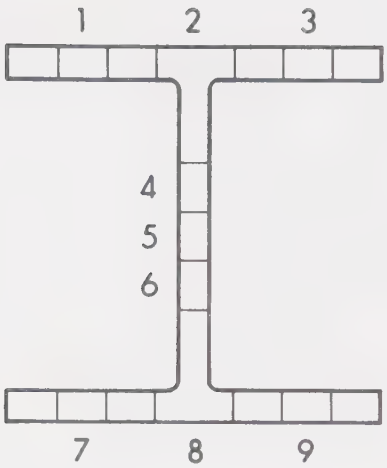

COUPON
LOCATIONS

Coupon	σ_y (ksi)	$\varepsilon_y=\sigma_y/E$*	ε_{st}	E_{st} (ksi)	σ_u (ksi)	Elongation %
1	53.4	0.0018	0.0126	741	81.7	21.0
2	--	--	--	--	81.7	21.5
3	54.4	0.0018	0.0120	527	81.9	20.3
4	61.9	0.0020	--	585	84.5	20.4
5	51.9	0.0017	0.0150	800	82.6	20.5
6	59.7	0.0020	--	587	82.2	20.2
7	53.9	0.0018	0.0120	728	81.7	19.5
8	--	--	--	--	81.9	21.1
9	54.6	0.0018	0.0130	729	82.3	20.2

Note: * E taken as 29.6×10^3 ksi

TABLE 3.3 MATERIAL PROPERTIES

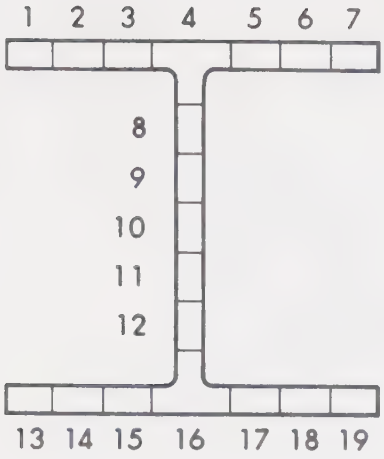

COUPON LOCATIONS

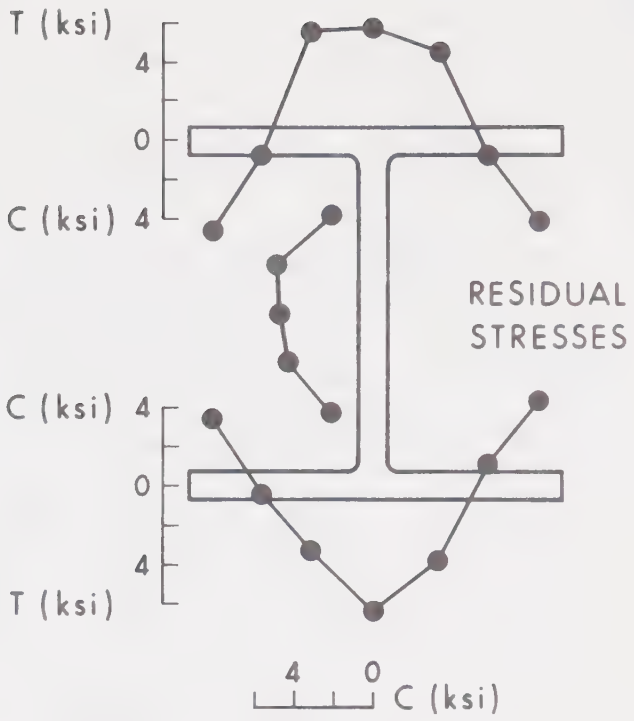

RESIDUAL STRESSES

Coupon	σ_y (ksi)	$\varepsilon_y=\sigma_y/E$*	ε_{st}	E_{st} (ksi)	σ_u (ksi)
1	53.5	0.00181	0.0172	542	81.0
2	48.2	0.00163	0.0182	848	81.3
3	51.3	0.00173	0.0172	737	82.9
4	46.9	0.00158	0.0140	327	76.5
5	48.2	0.00163	0.0170	752	82.4
6	52.6	0.00178	0.0174	767	81.9
7	53.1	0.00179	0.0196	771	81.8
8	51.9	0.00175	0.0146	607	82.6
9	52.9	0.00179	0.0166	720	84.2
10	53.7	0.00182	0.0184	714	82.4
11	51.1	0.00173	0.0160	711	81.8
12	51.5	0.00174	0.0152	763	83.7
13	52.4	0.00177	0.0186	912	82.4
14	50.7	0.00171	0.0170	790	81.6
15	47.5	0.00160	--	--	82.9
16	55.1	0.00186	0.0174	762	89.1
17	47.8	0.00162	0.0156	783	82.3
18	50.5	0.00171	0.0166	860	81.6
19	52.9	0.00179	0.0180	864	82.1

Note: E taken as 29.6×10^3 ksi

TABLE 3.4 MATERIAL PROPERTIES

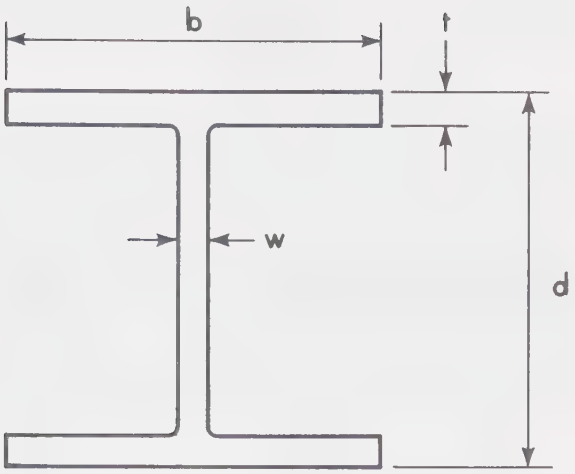

Section	d (in)	b (in)	t (in)	w (in)	I (in^4)	Z (in^3)	r_x (in)	A (in^2)
Typical	5.12	4.99	0.37	0.25	22.9	10.1	2.18	4.82
BC-9*	5.12	4.50	0.37	0.25	3.8	2.9	--	--

Note: * Upper beam bent about weak axis.

TABLE 3.5 CROSS-SECTION DIMENSIONS

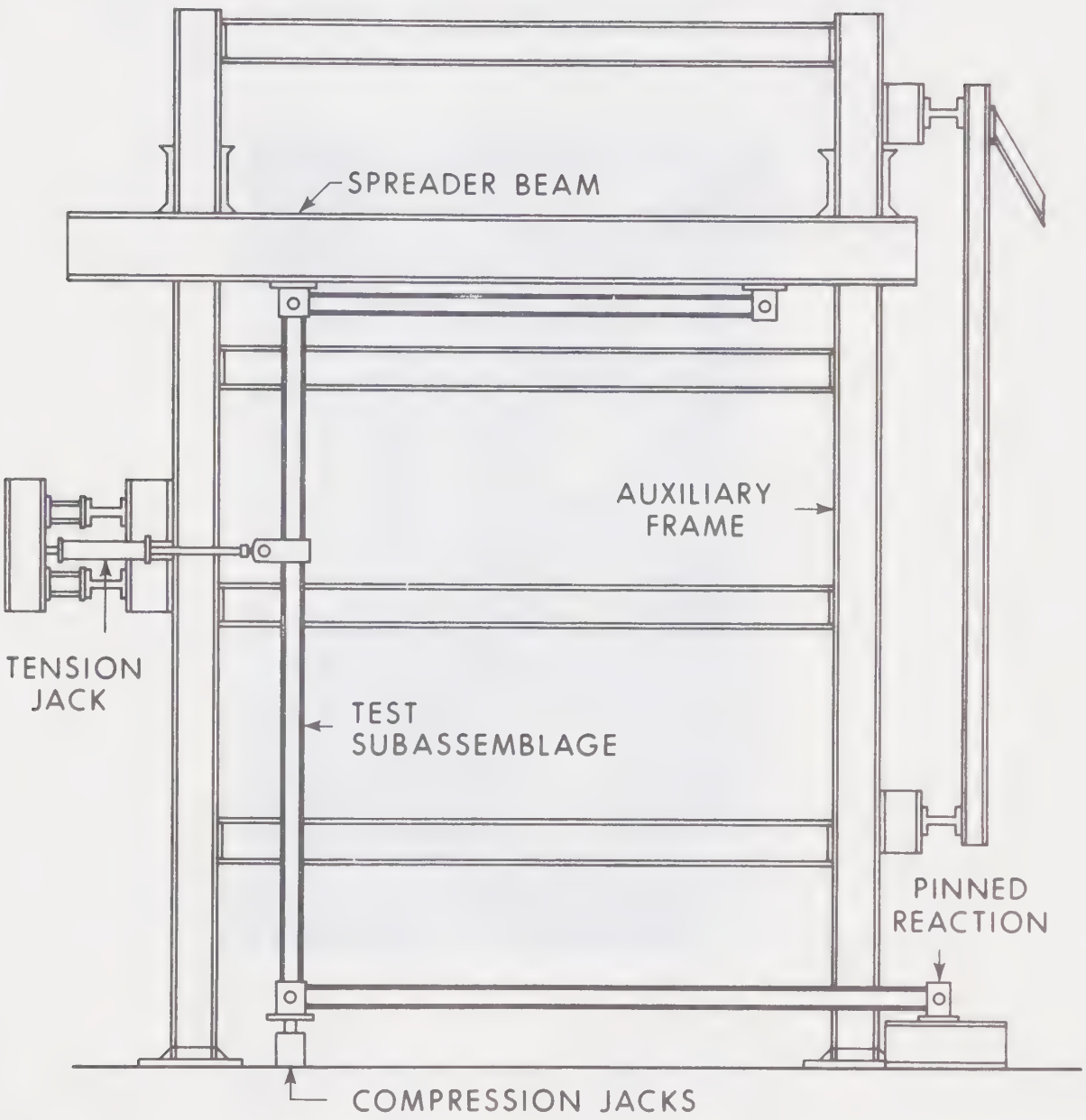

FIG. 3.1 TEST SET-UP

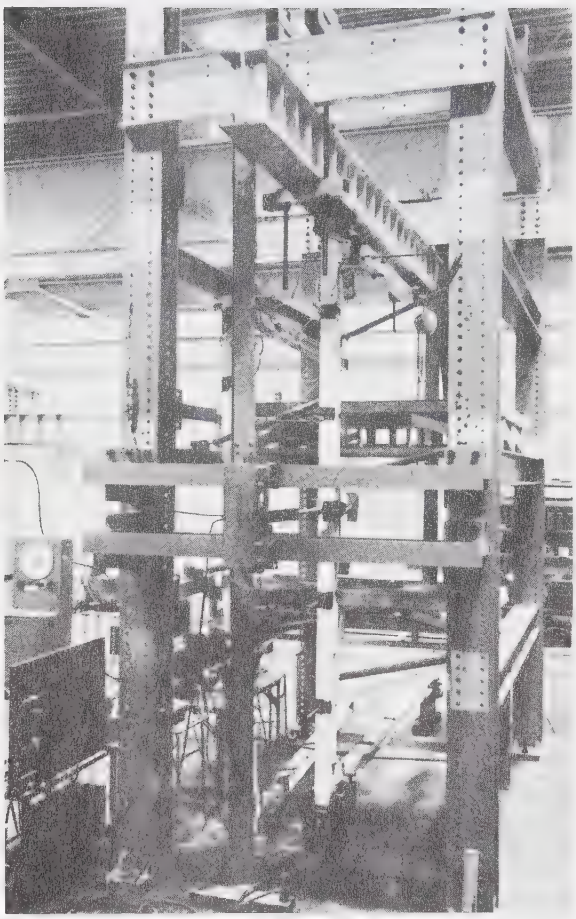

FIG. 3.2 OVERALL VIEW OF TEST SET-UP

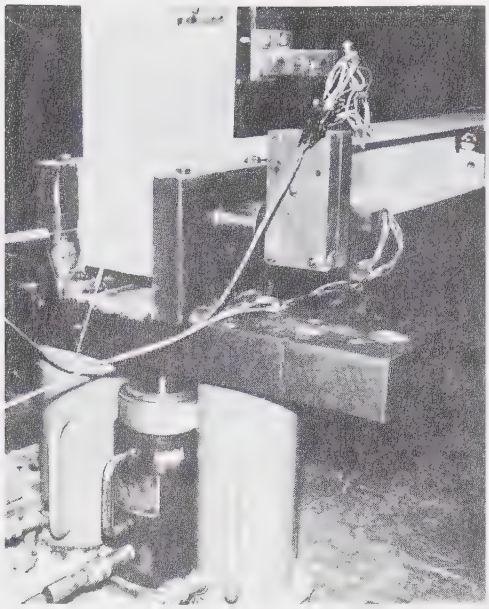

(a)

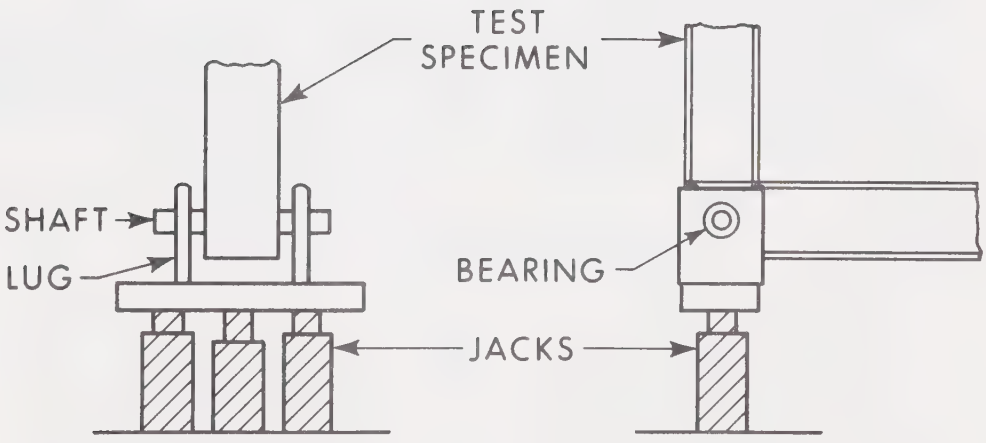

(b)

FIG. 3.3 VERTICAL LOAD APPLICATION

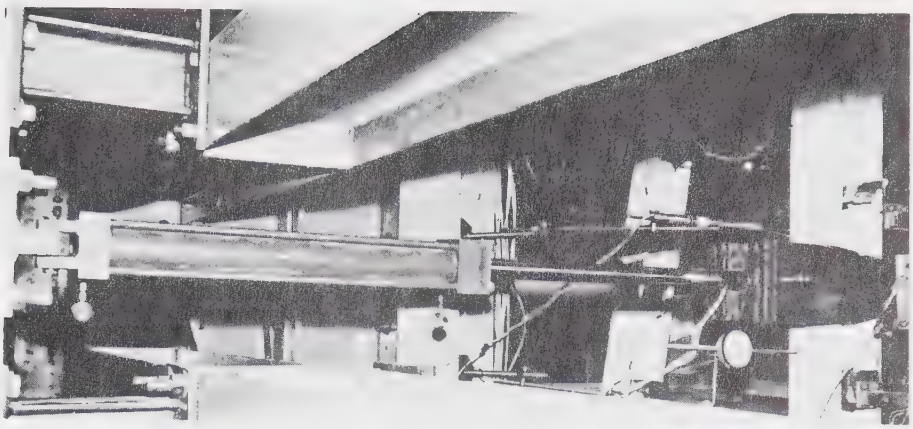

(a)

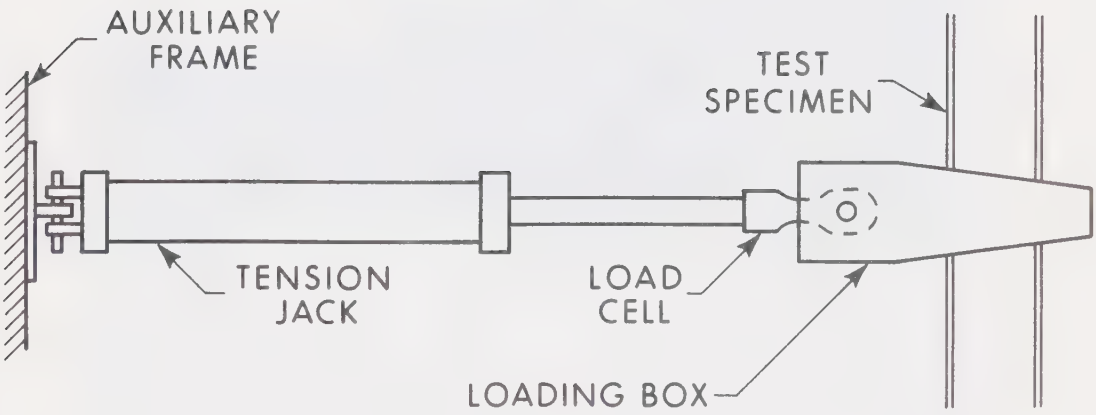

(b)

FIG. 3.4 LATERAL LOAD APPLICATION

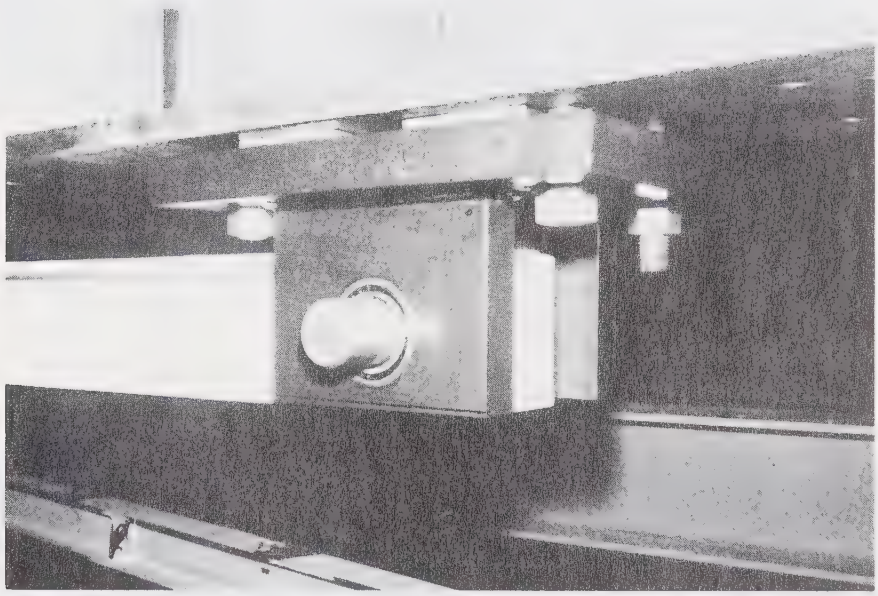

FIG. 3.5 RESTRAINING BEAM REACTION

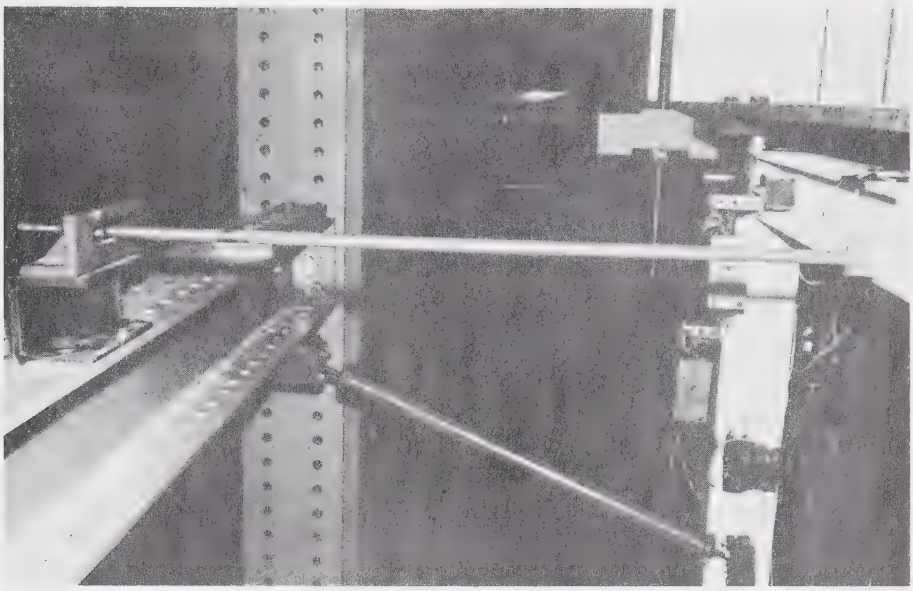

FIG. 3.6 LATERAL BRACE ON BEAM

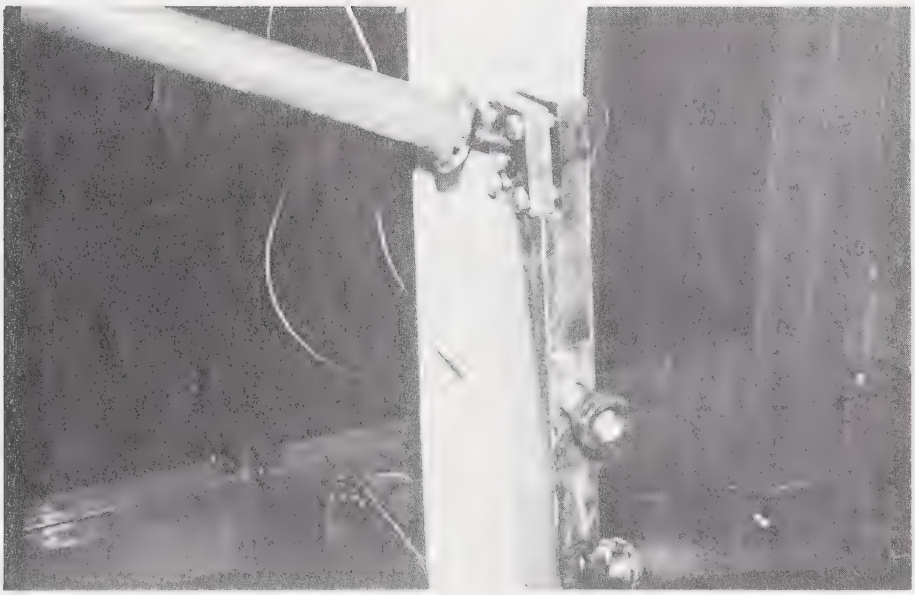

FIG. 3.7 ARTICULATED LATERAL BRACE ON COLUMN

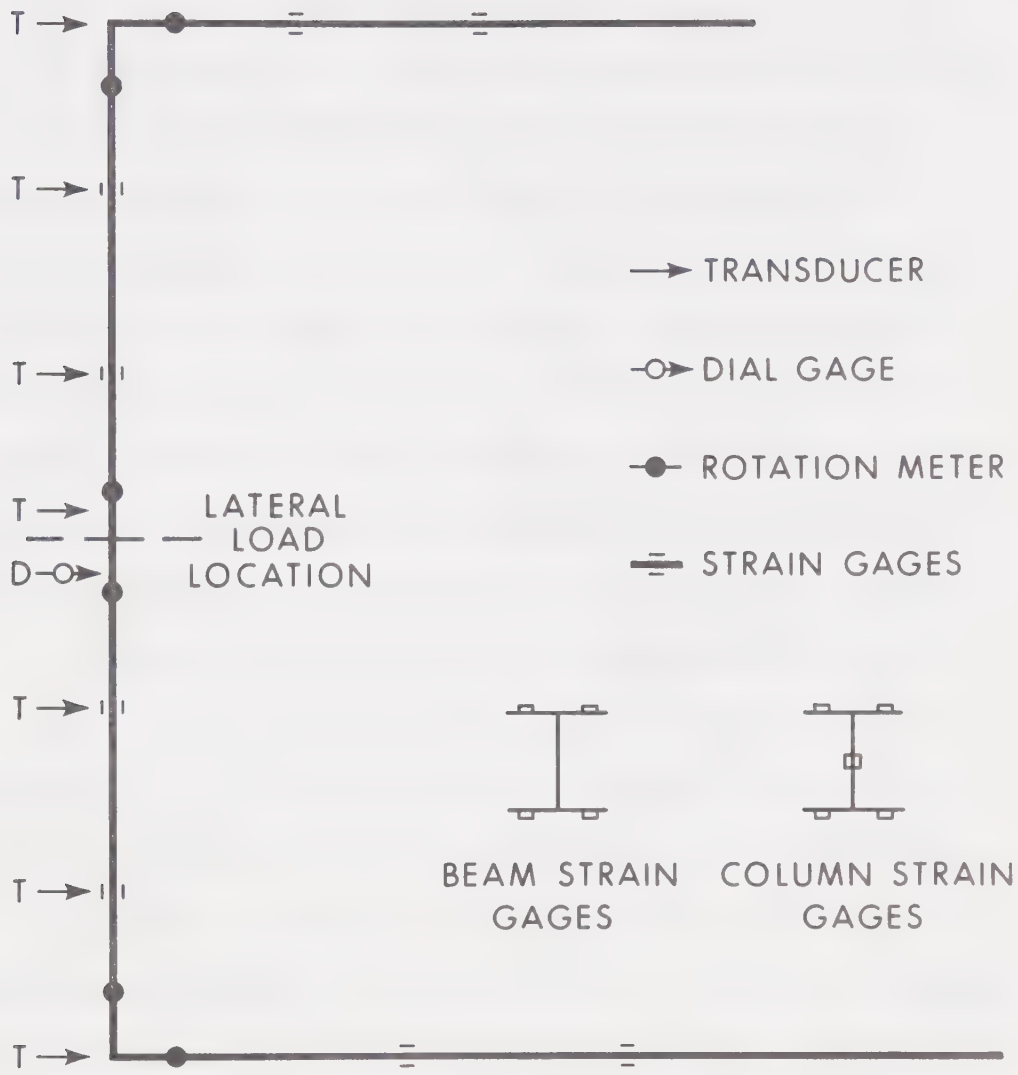

FIG. 3.8 INSTRUMENTATION

CHAPTER IV

TEST RESULTS

The results of tests on nine subassemblages are reported in this chapter. The subassemblages were subjected to non-proportional loading, the vertical loads on the columns were applied initially and held constant as the horizontal deflection at the load-point was gradually increased. After each deflection increment, the appropriate load, strain deflection and rotation readings were recorded and the specimen was inspected. The response of specimen BC-5 will be described in detail and the results of tests on the remaining subassemblages will be summarized briefly.

Test BC-5 was performed on a restrained beam column with a slenderness ratio, $L/r_x = 78$. The relative beam to column stiffness, G_u, at the upper joint was 0.47 and at the lower joint $G_l = 0.66$. The dimensions of the specimen are listed in TABLE 3.1. The lateral load was applied at mid-height of the column and the column was subjected to a vertical load of 130 kips, corresponding to $P/P_y = 0.53$.

The response of subassemblage BC-5, as characterized by the R-Δ curve, is shown in FIG. 4.1, where R is the lateral load and Δ is the deflection at the point of lateral load application. In FIG. 4.1 and the figures that follow, solid lines joining full circles will be used to denote test results and dashed lines will denote the theoretical predictions. The numbers adjacent to the full circles indicate stages at which data was taken during the test.

All the plotted points, including those on the descending portions of the curve, represent points at which the frame was in static equilibrium. The specimen response was predicted using a second order elastic-plastic calculation, which accounted for the actual hinge location and the increased strength due to strain-hardening. The procedure is described in APPENDIX D.

Loads Nos. 1 through 3 represent stages during which the vertical load was increased on the specimen. During the initial application of horizontal load, (load Nos. 3 to 5) the frame response followed that predicted assuming elastic behavior. At load No. 5, initial yielding was observed on the compression flange of the column adjacent to the lateral load-point and minor yielding was also observed at the beam-to-column connections. As loading progressed (load Nos. 5 to 7) yielding spread along the compression flange of the beam-column at the load-point. In addition, between load Nos. 6 and 7, yielding was initiated at points approximately seven inches above and below the load-point, on the compression flange of the beam-column. FIG. 4.2 (b) indicates the extent of yielding adjacent to the load-point at this stage, while FIGS. 4.2 (a) and (c), show the minor yielding adjacent to the top and bottom beam-to-column connection, respectively. Beyond load No. 7 the yielding of the compression flange at the load-point propagated along the length of the column from locations approximately seven inches below and above the load-point; yielding also spread from the load-point stiffener. At load No. 9, yielding of

the web at the load-point was first observed; this yielding quickly spread and extended approximately nine inches above and below the stiffener. Also at load No. 9, increased yielding was observed adjacent to the beam-to-column connections. Yielding at these locations developed in the same manner as described for the load-point area; that is, immediately after the start of increased yielding at the stiffener, a second yielding pattern started at some distance away (approximately three inches at the top of the column and approximately seven inches at the bottom) and as the deflection increased, yielding spread both from the stiffener and from the second yielded zone. The ultimate lateral load, R_{max}, was obtained at load No. 12 and was equal to 7.8 kips. Beyond this stage unloading occurred with increasing deflections. FIGS. 4.3 (a), (b) and (c) show the extent of yielding observed at load No. 13, immediately after the attainment of the ultimate load. At load No. 18, the test was terminated. FIGS. 4.4 (a) through (f) show the extent of yielding of both the compression flange and web at the load-point and connections, at this stage. A local buckle of the compression flange at the load-point was observed at load No. 18 with a half wave forming on each side of the load-point stiffener. The center of each half was located approximately seven inches from the load-point. Lateral deformations of the column were not observed. Between load Nos. 18 and 19, the lateral load was removed and between load Nos. 19 and 20, the axial load was removed. FIG. 4.5 shows an overall view of the specimen after the

test had been completed.

The internal bending moments at two locations on each member segment were determined from strain gage readings. For the restraining beams these values were extrapolated directly to predict the bending moment at the beam-to-column connections. For the column segments, since the deflections were measured, the secondary bending moments could be determined and the moments were computed at the segment ends. The bending moments at various critical locations are plotted against the load-point deflections in FIG. 4.6, the arrows indicate stages at which the (modified) reduced plastic moment capacities of the columns are attained.

The response of test BC-5, described above in detail, was generally typical of the responses of the subassemblages tested. The maximum ultimate load, R_{max}, obtained in each of the tests, as well as the important parameters involved, are listed in TABLE 4.1. FIGS. 4.7 through 4.15 show the R-Δ curves for all specimens. In these figures, R has been non-dimensionalized by R_{pc}, the lateral load capacity predicted by simple plastic theory (the plastic moment capacities of the columns are modified for the presence of axial load). A summary of the visual observations noted during these tests is given in TABLE 4.2.

For the specimens loaded at mid-height, the maximum moment in the central portion of the column occurred at the load-point. For the specimens loaded at the upper third-point, however, the maximum secondary moments occurred below the load-point. In

spite of this, for the stocky specimens (BC-8 and BC-9) the maximum total moment occurred at the load-point. For BC-7, which was slender and subjected to a high axial load, the secondary moments were more significant and extensive yielding was observed below the load-point and eventually a local buckle formed in this area. FIG. 4.16, shows the bending moment distributions for this specimen at the beginning of inelastic action, load No. 8. In FIG. 4.16, the points indicated are the total moments determined from the measured strains; the curve, representing the distribution, was estimated and indicates that the point of maximum bending moment occurred below the load-point.

Test	P (kips)	P/P_y	L/r_x	R_{pc} (kips)	R_{max} (kips)
BC-1	64	0.26	78	10.2	7.4
BC-2	63	0.26	110	15.1	11.1
BC-3	110	0.45	110	11.2	5.0
BC-4	73	0.30	78	18.4	20.1
BC-5	130	0.53	78	13.5	7.8
BC-6	64	0.26	110	16.9	12.9
BC-7	111	0.45	110	12.5	6.6
BC-8	73	0.30	78	22.6	20.8
BC-9	73	0.30	78	17.7	15.3

TABLE 4.1 ULTIMATE STRENGTHS OF SUBASSEMBLAGES

TEST	HINGE SEQUENCE		CONCENTRATION OF YIELDING			BUCKLING			
	PREDICTED	OBSERVED	LOAD-POINT	COLUMN TOP	COLUMN BOTTOM	LOCAL			LATERAL
			DISTANCE FROM LOAD-POINT x_1 (in.)	DISTANCE FROM FACE OF CONNECTION x_2 (in.)	DISTANCE FROM FACE OF CONNECTION x_3 (in.)	LOAD No.	DISTANCE DOWN FROM LOAD-POINT x_4 (in.)	LENGTH OF QUARTER WAVE x_5 (in.)	LOAD No
				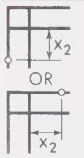			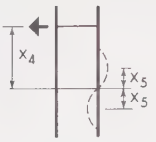		
BC-1			8			18	0	5	18
BC-2	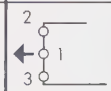	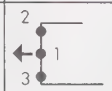	7	8	8	33	0	7	33
BC-3	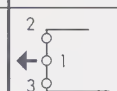	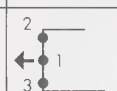	7	-	-	24	0	6	25
BC-4	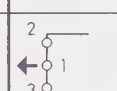	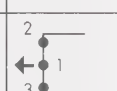	7	4	4	22	0	4	22
BC-5	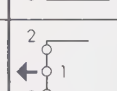	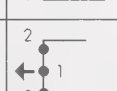	7	3	7	18	0	5	
BC-6	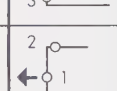	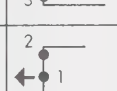	7	8					
BC-7	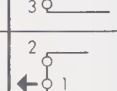	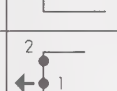	*	8	8	17	24	4	18
BC-8	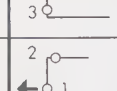		6	6	4	23	9	5	20
BC-9	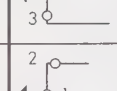		8	6	-	23	10	3	18

Note: * Yielding developed well below load-point.

TABLE 4.2 VISUAL OBSERVATIONS

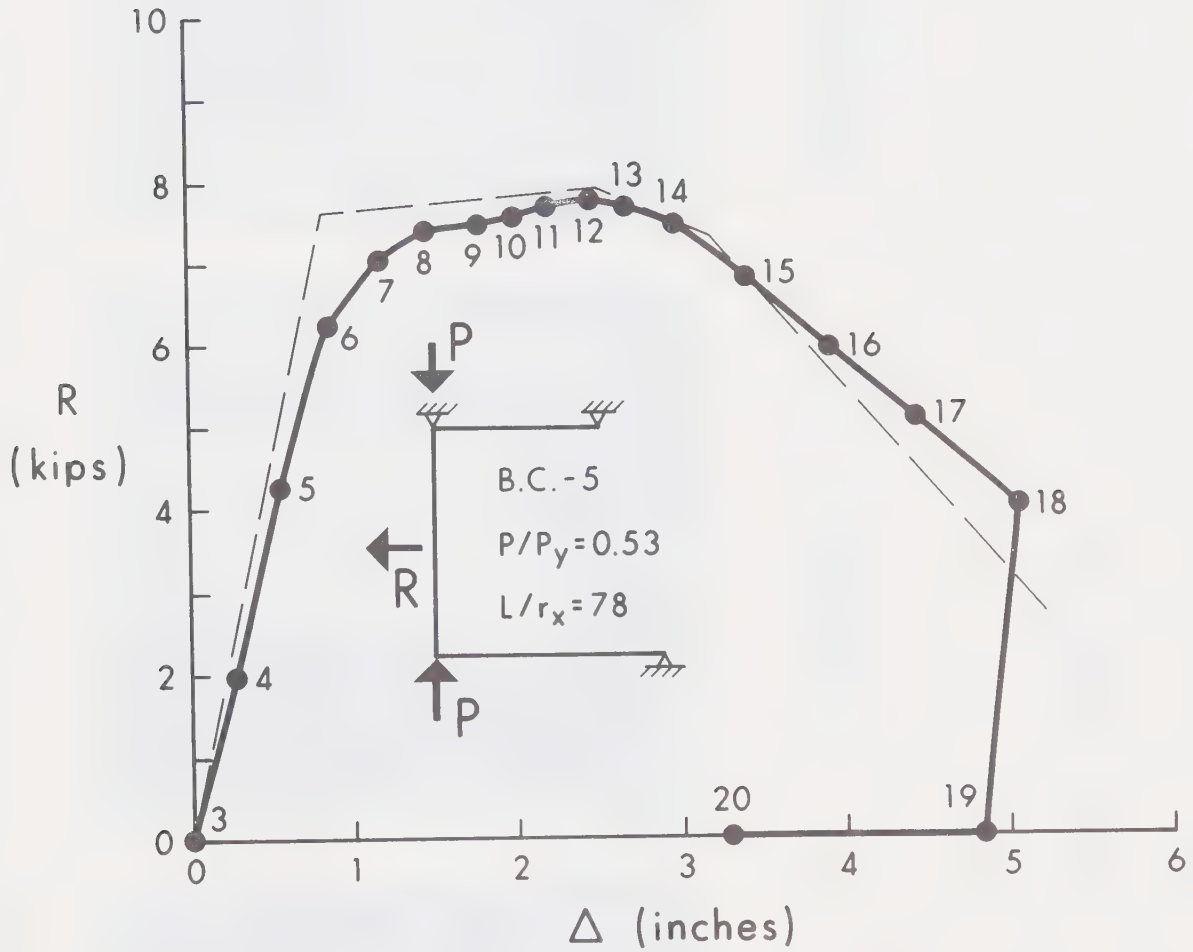

FIG. 4.1 LOAD-DEFLECTION RELATIONSHIP - BC-5

(a) Top of column (compression flange)

(b) Load-point (compression flange)

(c) Bottom of column (compression flange)

FIG. 4.2 YIELDED ZONES - BC-5 - LOAD NO. 7

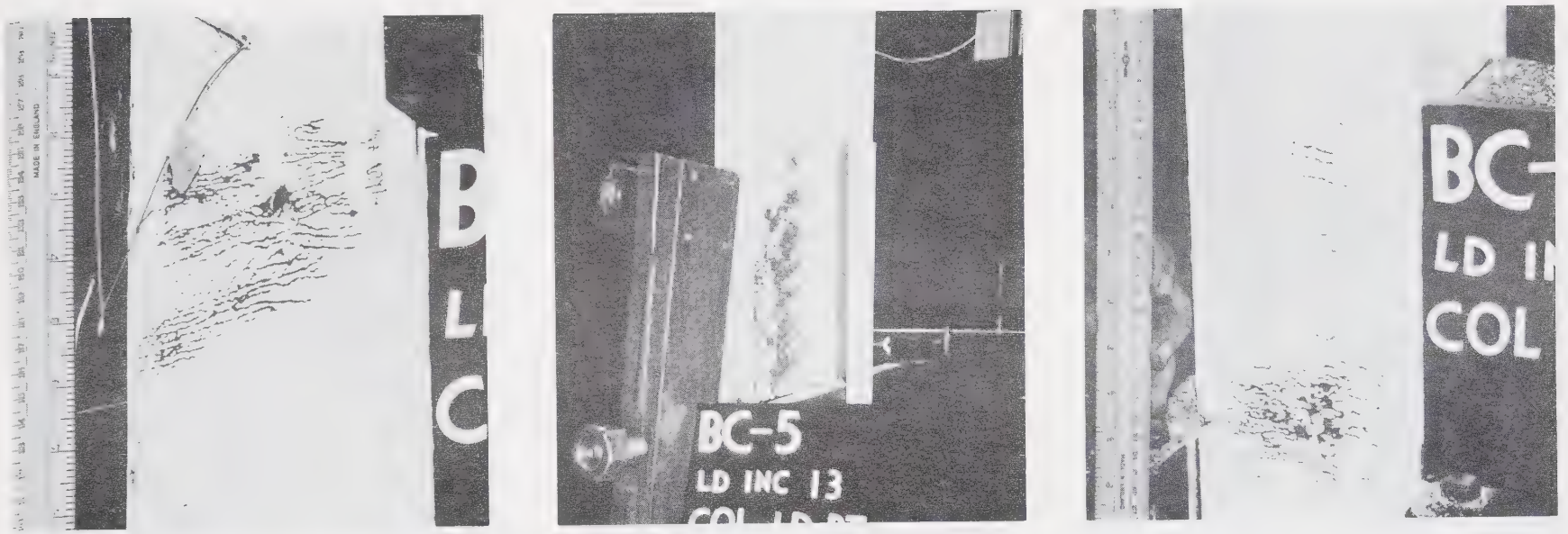

(a) Top of column (compression flange)

(b) Load-point (compression flange)

(c) Bottom of column (compression flange)

FIG. 4.3 YIELDED ZONES - BC-5 - LOAD NO. 13

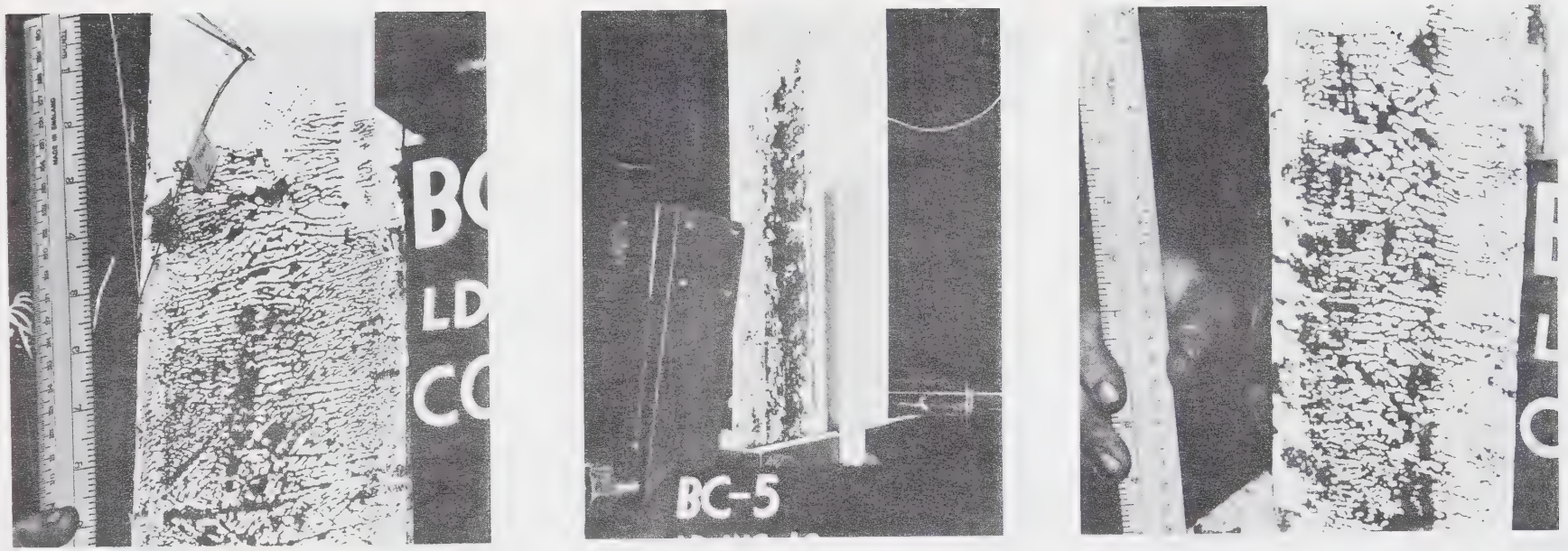

(a) Top of column (compression flange)

(b) Load-point (compression flange)

(c) Bottom of column (compression flange)

FIG. 4.4 YIELDED ZONES - BC-5 - LOAD NO. 18

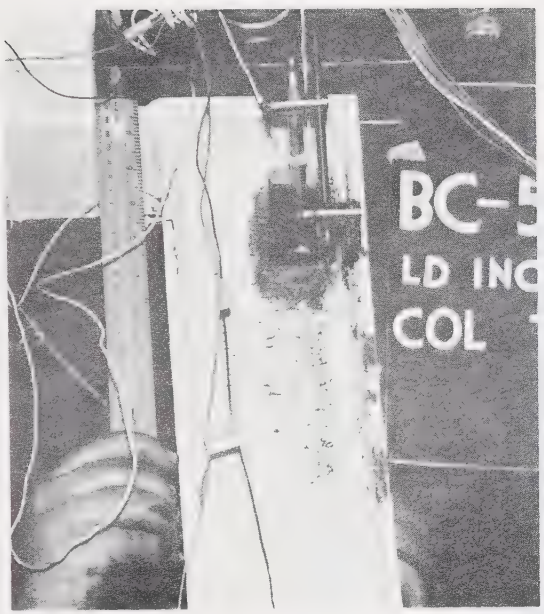

(d) Top of column (web)

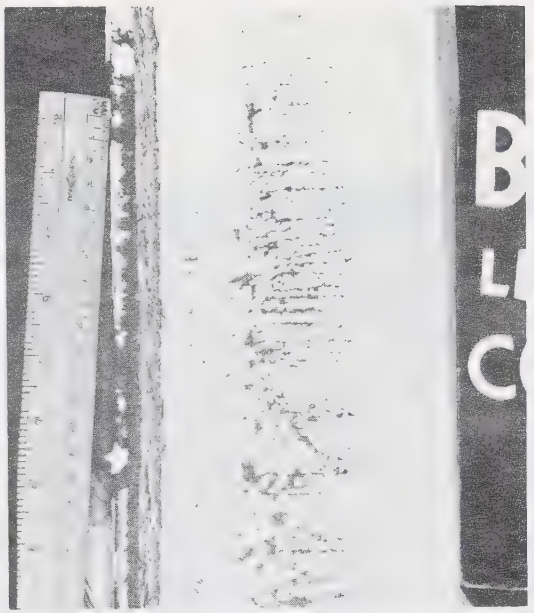

(e) Load-point (web)

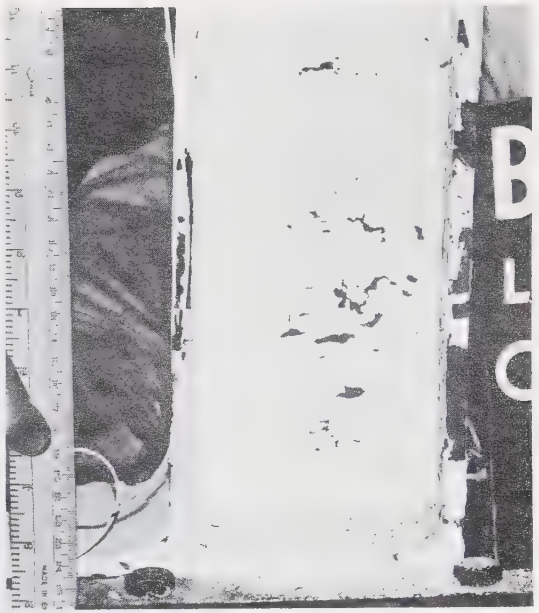

(f) Bottom of column (web)

FIG. 4.4 YIELDED ZONES - BC-5 - LOAD NO. 18 (cont'd)

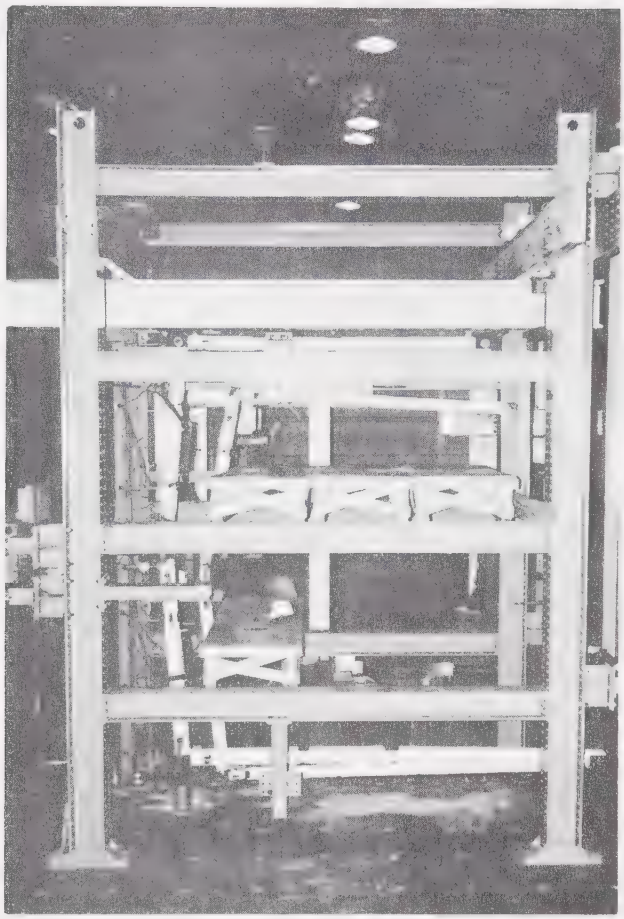

FIG. 4.5 BC-5 AFTER TESTING

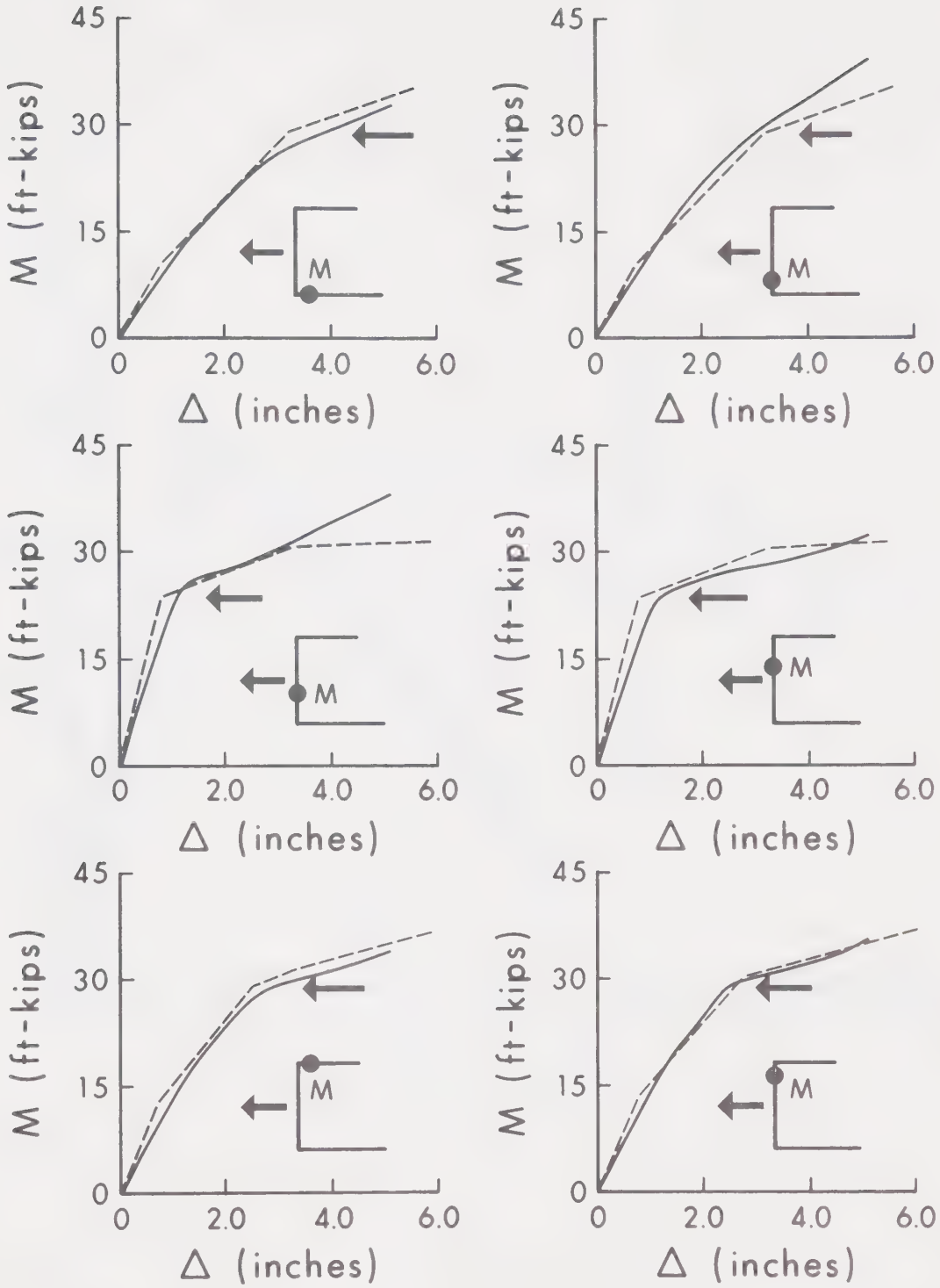

FIG. 4.6 BENDING MOMENT-DEFLECTION RELATIONSHIP - BC-5

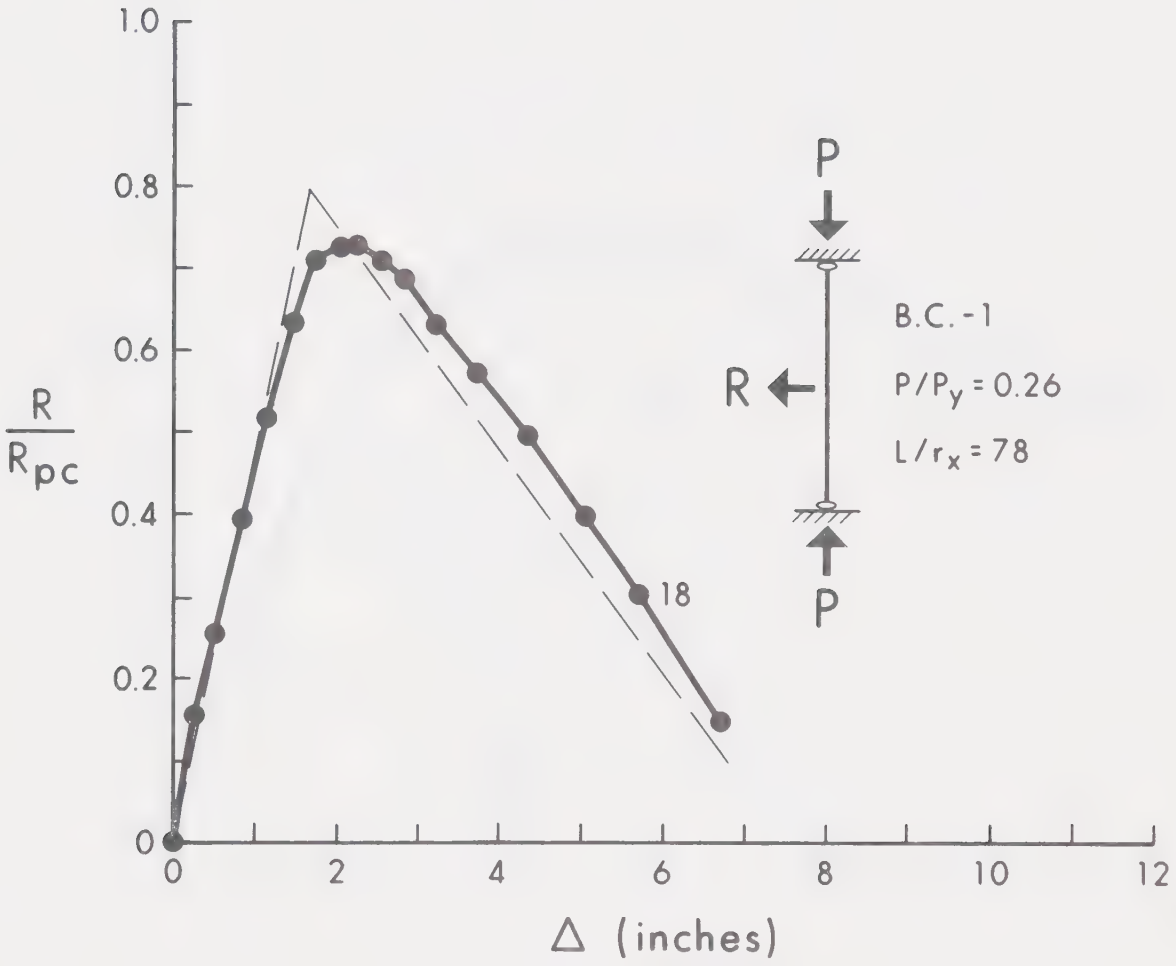

FIG. 4.7 LOAD-DEFLECTION RELATIONSHIP - BC-1

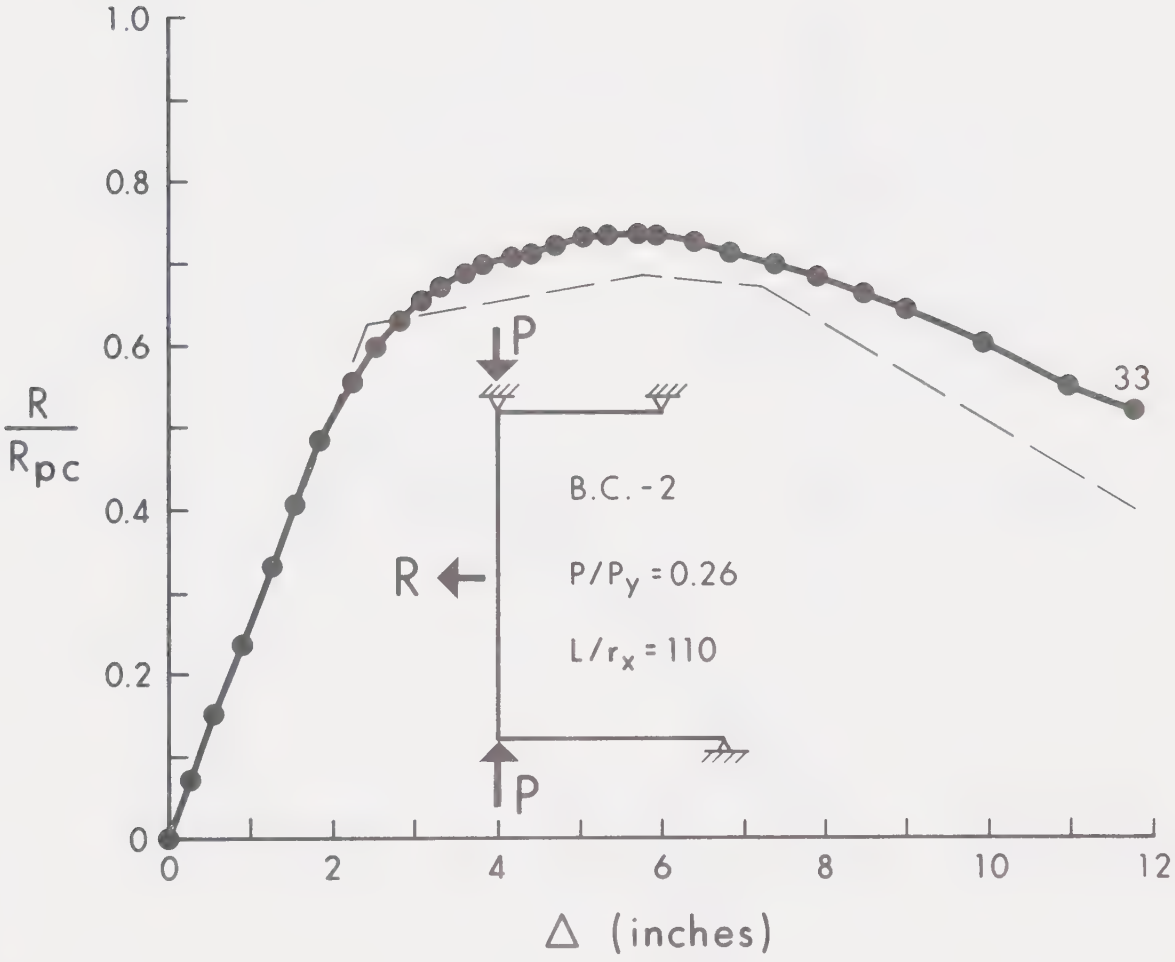

FIG. 4.8 LOAD-DEFLECTION RELATIONSHIP - BC-2

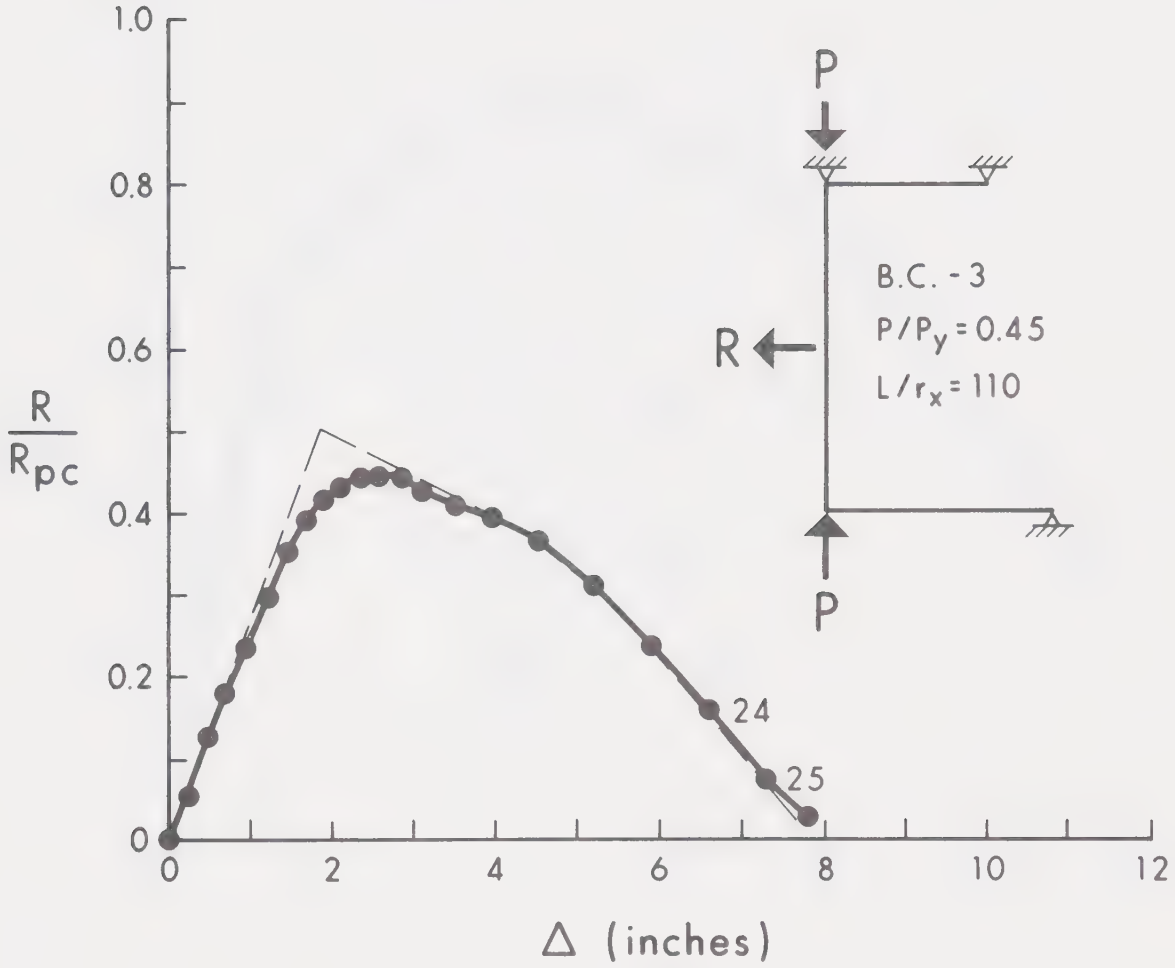

FIG. 4.9 LOAD-DEFLECTION RELATIONSHIP - BC-3

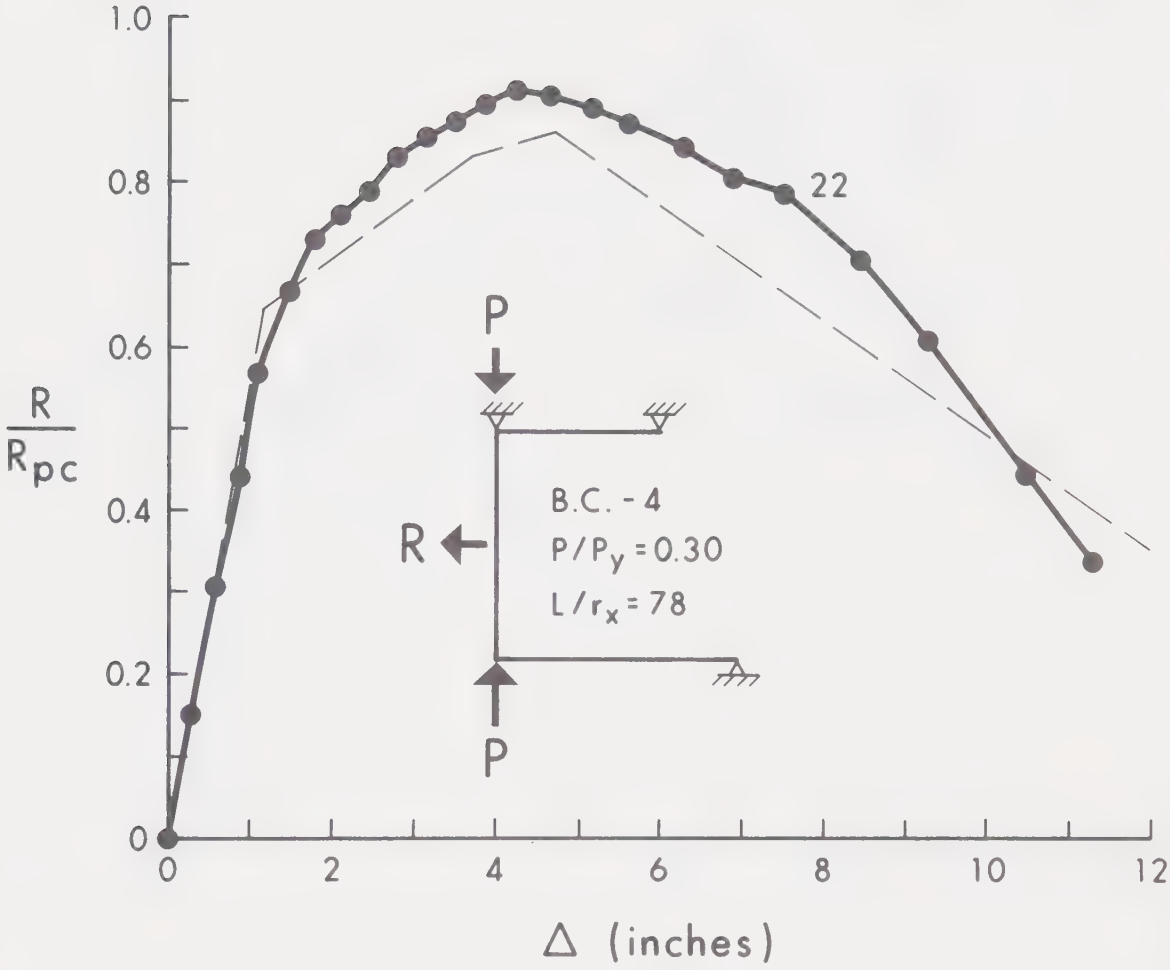

FIG. 4.10 LOAD-DEFLECTION RELATIONSHIP - BC-4

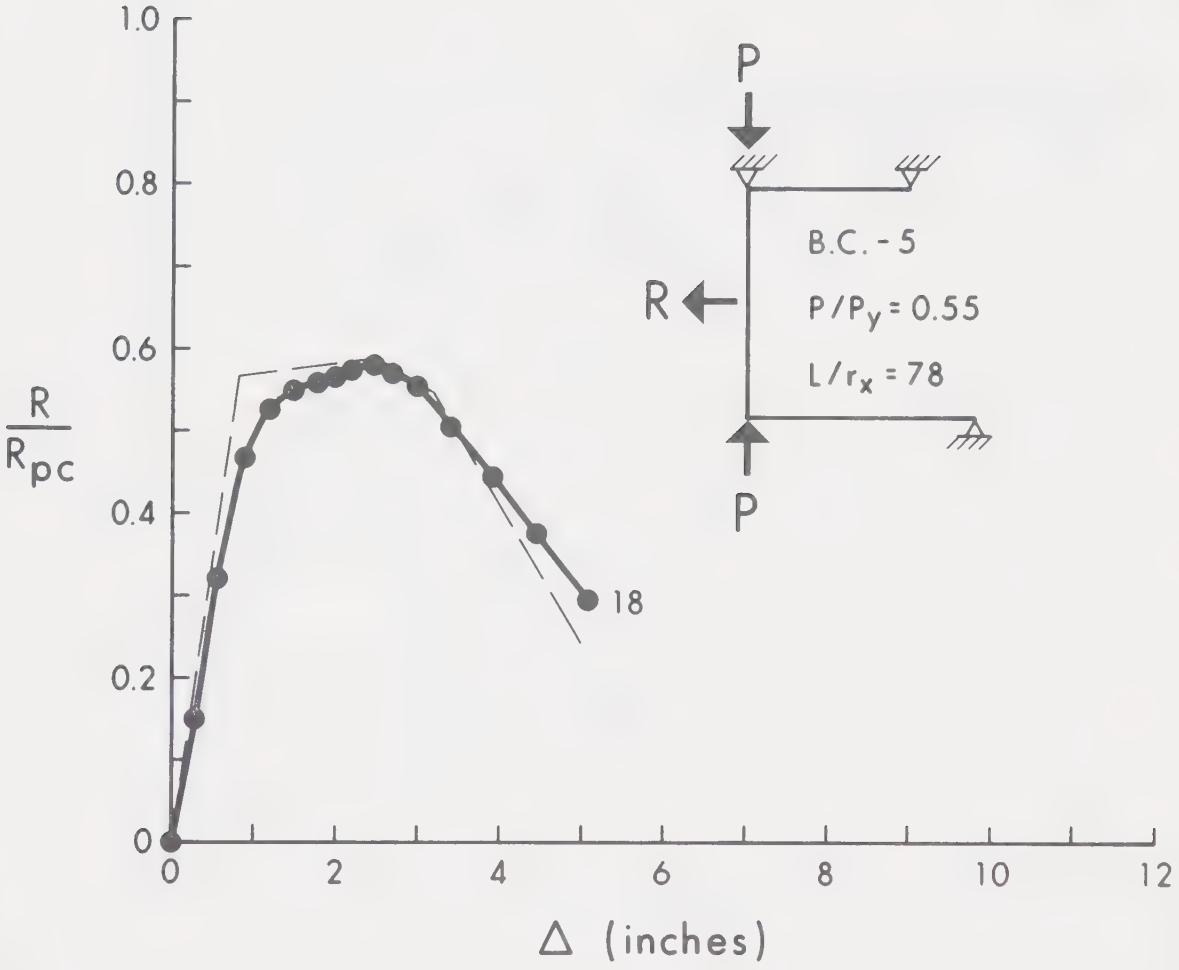

FIG. 4.11 LOAD-DEFLECTION RELATIONSHIP - BC-5

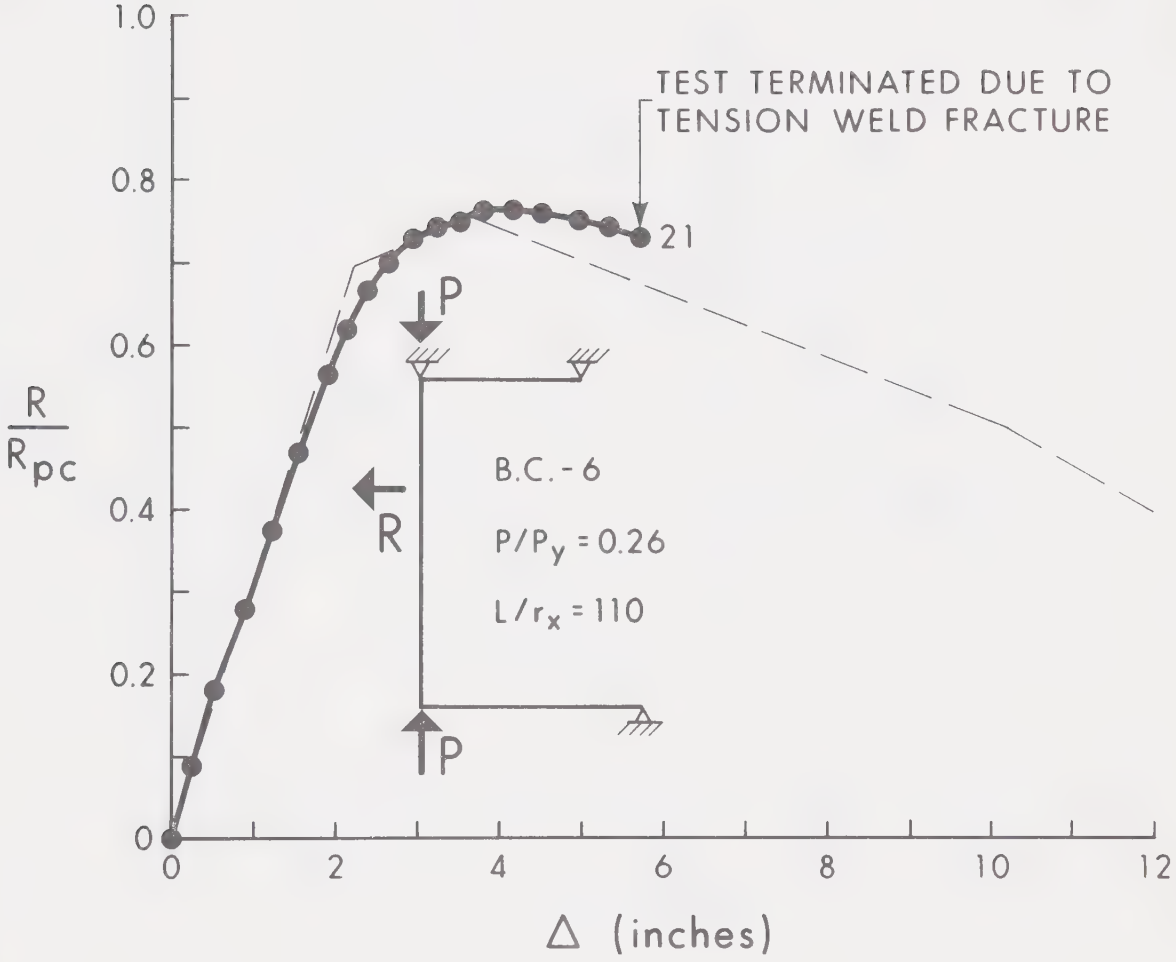

FIG. 4.12 LOAD-DEFLECTION RELATIONSHIP - BC-6

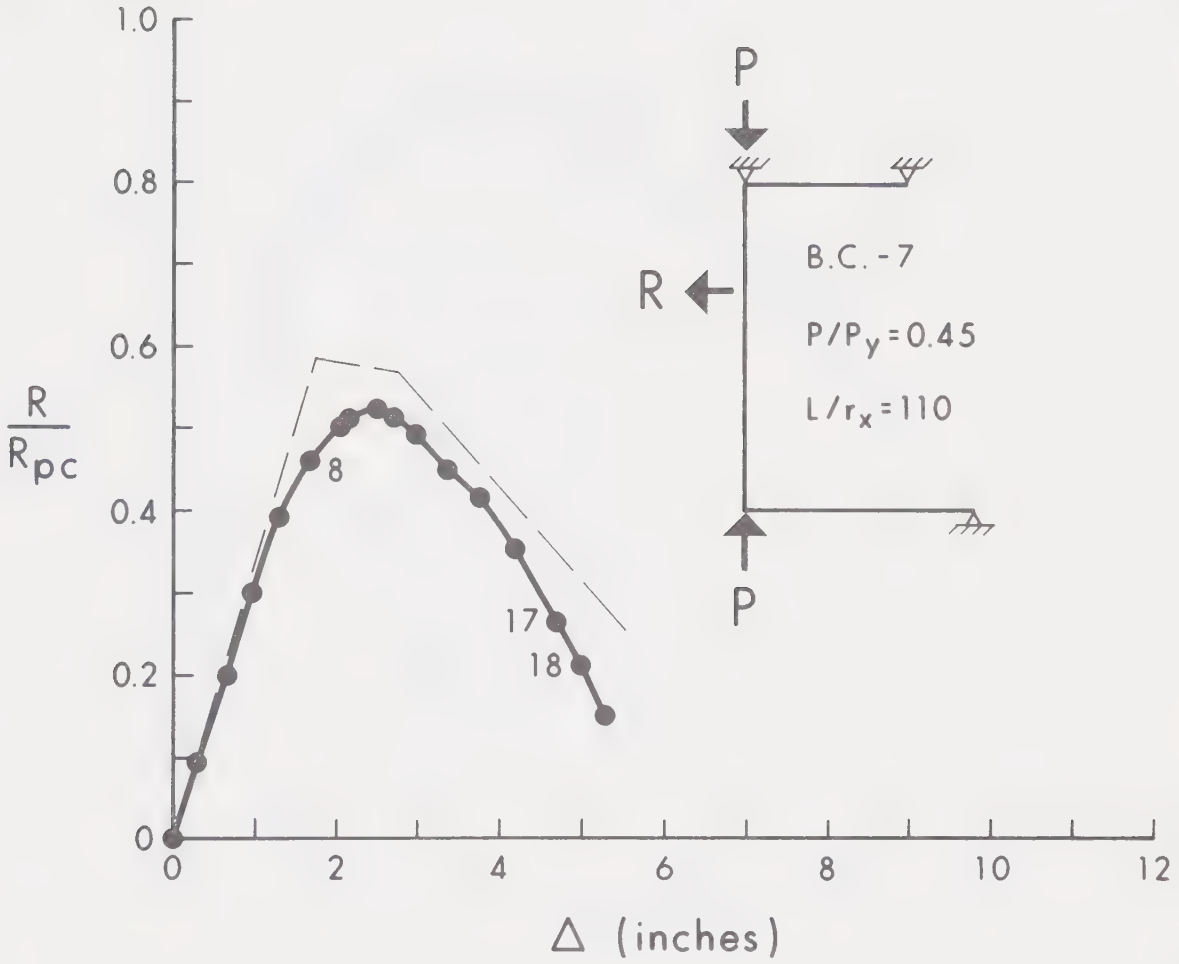

FIG. 4.13 LOAD-DEFLECTION RELATIONSHIP - BC-7

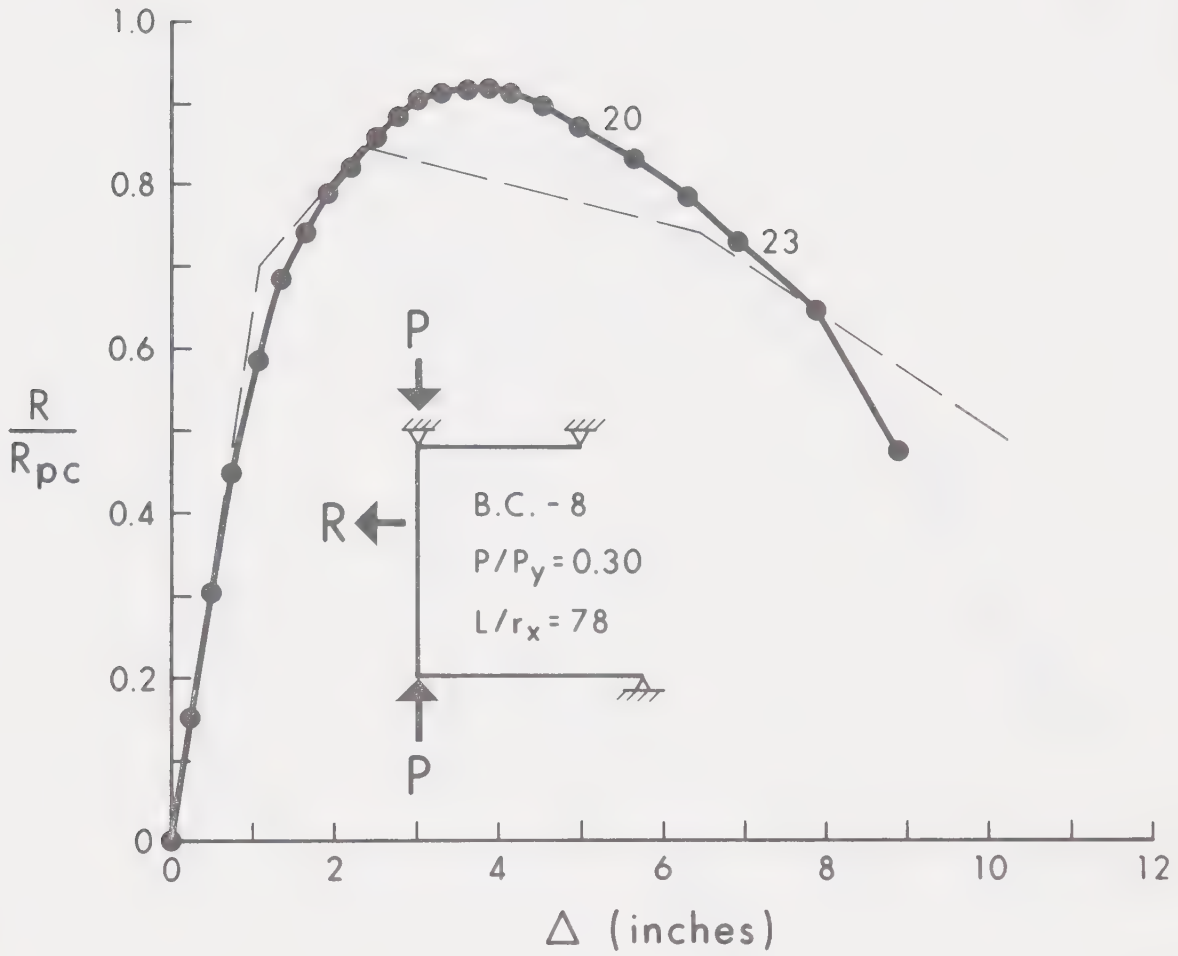

FIG. 4.14 LOAD-DEFLECTION RELATIONSHIP - BC-8

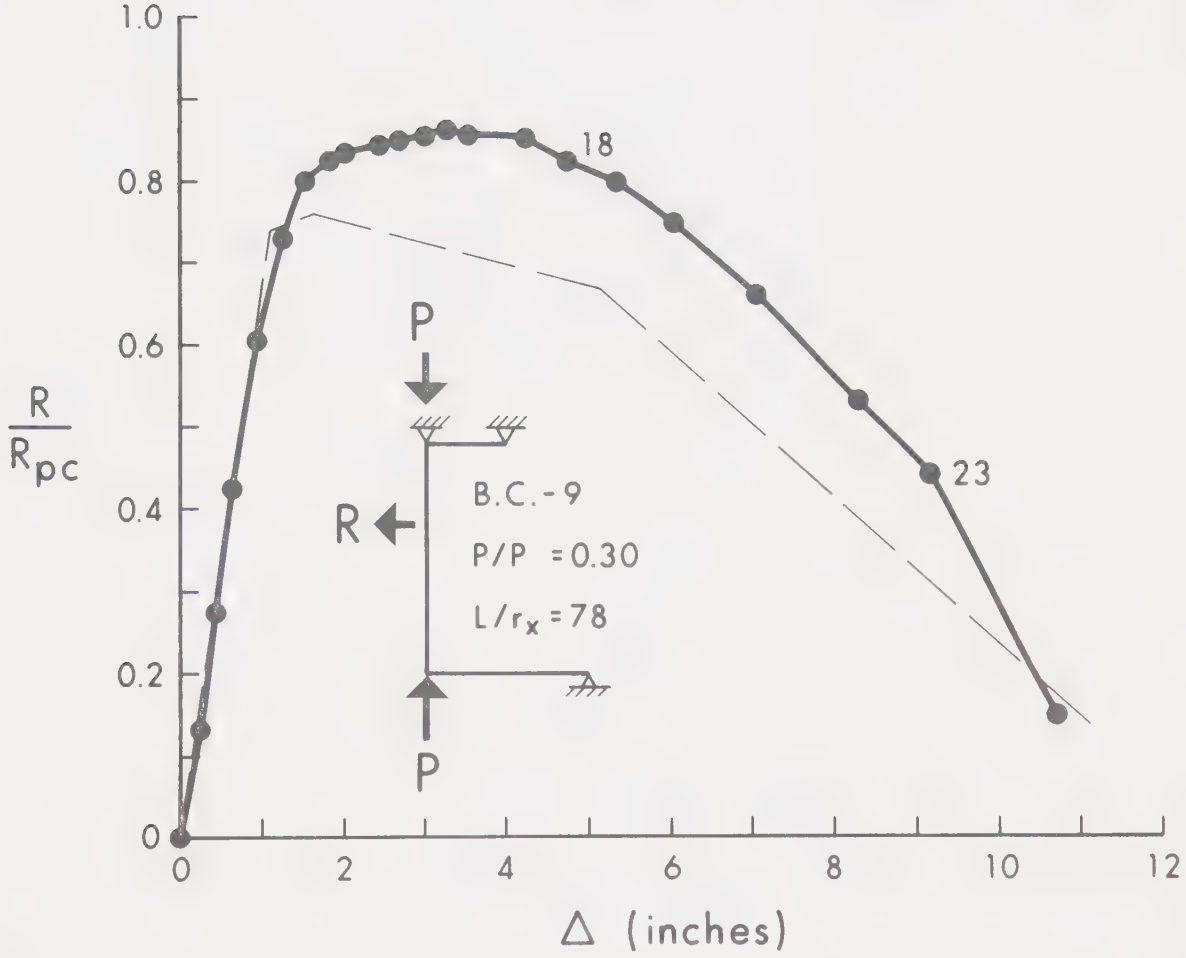

FIG. 4.15 LOAD-DEFLECTION RELATIONSHIP - BC-9

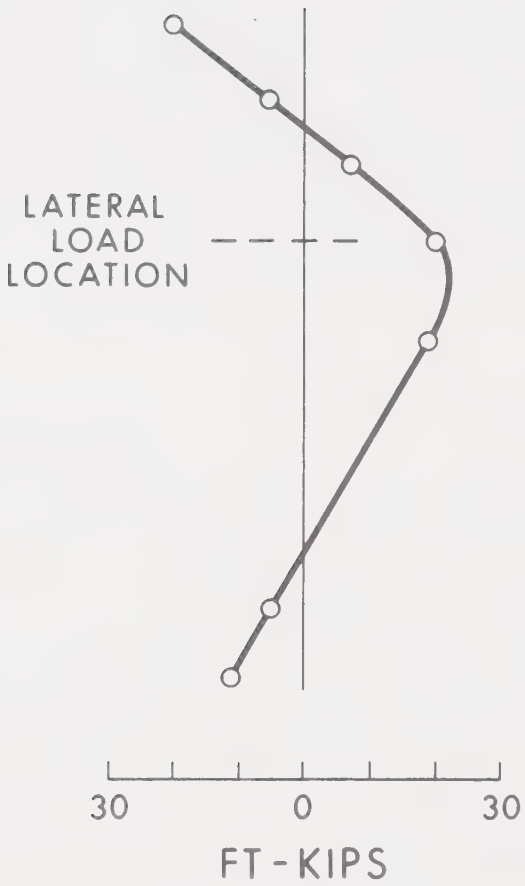

FIG. 4.16 BENDING MOMENT DISTRIBUTION - BC-7 - LOAD NO. 8

CHAPTER V

DISCUSSION OF TEST RESULTS

Introduction

The results of tests performed on nine laterally loaded subassemblages have been presented in the previous chapter. In this chapter, the observed behavior will be discussed and compared with that predicted on the basis of elastic-plastic member behavior. The ultimate carrying capacities determined from the tests will also be compared with those predicted by the modified interaction equations (4).

Behavior of Test Subassemblages

Generally, the trends shown by the experimental results agreed with those predicted; the shapes of the load-deflection curves, the hinge sequence and the general behavior of the specimens were as predicted by the second-order elastic-plastic analysis.

The initial portions of the observed load-deflection curves were almost exactly as predicted by the analysis. At this stage the behavior of the subassemblages appeared to be elastic. Yielding of the compression flange at the load-point stiffener occurred at loads approximately half of those corresponding to the predicted formation of the first hinge. This was possibly due to the increased residual stresses at these locations due to welding. The yielding pattern was localized and apparently had little effect

on the overall stiffnesses of the subassemblages.

At lateral loads approximately two-thirds of those corresponding to the predicted formation of the first hinge, yielding occurred in the vicinity of the load-point. (In all cases, the first hinge was predicted at the load-point.) As the predicted first hinge load level was approached, increased yielding occurred in the region of the load-point and the stiffnesses of the subassemblages gradually decreased. This gradual decrease in stiffness was due to the combined effects of residual strains and applied moments. This action produced a smooth transition between the branches of the load-deflection curves.

As predicted, the first hinge formed in the vicinity of the load-point. In most cases, yielding was concentrated at some distance away from the load-point stiffener; this distance varied from d to 1.5d, where d denotes the depth of the member. (It has been reported previously that at rigidly framed connections, the plastic hinging area is forced out into the member by a distance d from the face of the connection (14)). This effect at the stiffener, however, was not anticipated and was not included in the prediction. For test B.C.-7, however, which was loaded at the upper third-point, the yielded zone developed well below the load-point, apparently at the point of maximum moment.

Up to the formation of the first hinge, the bending moments at the load-point and the connections, balanced to within

five percent. In all cases except for BC-7, the maximum moment occurred at the load-point;in test BC-7, FIG. 4.16 indicates that the maximum moment occurred at some distance away from the load-point.

With increased deflections (after the formation of the first hinge), the yielded zones spread along the member length. Inelastic action was then observed at the upper beam-to-column connection as predicted. For all restrained tests except BC-6, yielding was observed in either the column or beam, as predicted, however, in BC-6 the hinge was predicted in the beam but the first significant yielding was observed in the column. The hinges formed at distance d to 1.5d away from the face of the connection (d was assumed in the prediction).

With increased deflections after the formation of the second hinge, yielding spread from both the load-point and upper connection areas. For all restrained tests except BC-6 and BC-7, inelastic action was observed in the column above the lower beam-to-column connection, as described above for the upper connection. Test BC-6 had been terminated due to a tension weld fracture, immediately after the formation of the second hinge and test BC-7 was terminated because of large deflections before the third hinge had formed. In both cases, the ultimate load capacity for the specimen had been attained.

For all tests, the spread of the plastic hinging areas considerably influenced the behavior. The existence of large yielded zones adjacent to plastic hinges implied that the moments at the connections and load-points were considerably in excess of the plastic moment capacities (14). The moments in these regions

extrapolated from strain measurements, were in excess of the reduced plastic moment capacities at the onset of major yielding and increased throughout the major portion of the test. This effect was included in the prediction; FIG. 4.6 compares the observed and predicted moments for test BC-5 and the agreement confirms the significant effect of strain-hardening in these tests.

The maximum loads observed during the tests were within twelve percent of those predicted. TABLE 5.1 summarizes the maximum loads for the nine tests. The ratio of the maximum loads observed to that predicted ranges from 0.91 to 1.12 with a mean value of 1.01. For tests BC-1 and BC-3, the formulation of the first hinge coincided with the maximum capacity of the subassemblage. In these tests, the effect of the residual strains and the gradual penetration of yielding would significantly reduce the predicted maximum capacities. For test BC-7, the large secondary moments caused the plastic hinge in the column to form below the load-point; this possibility was not accounted for in the analysis and possibly accounts for the high value of the predicted ultimate load. For tests BC-8 and BC-9, which contained one very short column segment, the assumption that the plastic hinge formed at the load-point resulted in a prediction which considerably underestimated the load capacity of these columns.

Local and lateral buckling occurred only towards the end of the tests, after the ultimate capacities had been reached and considerable unloading had occurred. The local buckle formed in one complete wave; for those specimens subjected to mid-point loading, a half wave formed on each side of the load-point stiffener; in the

cases of upper third-point loading the wave formed below the load-point. Lateral deflections generally followed local buckling but occurred so late in the tests, that it was often impossible to deflect the specimens further to determine the effect of out of plane deflections.

Comparision of Experimental Results and Interaction Equations

The maximum lateral loads observed from the tests were compared with those predicted using the interaction equations (4). In this technique the member is divided into two segments at the point of load application and each segment is treated as a member which depends on its own flexural stiffness to prevent sidesway. An equivalent moment factor, $C_m = 0.85$, is used in conjunction with the maximum end moment on each segment. However, in computing the slenderness ratio, the total length of the member is used. For the test specimens, the maximum moment, M, corresponds to the maximum lateral load; the actual yield stresses and section properties were used to compute M_p and P_y.

The first equation is given by:

$$\frac{P_f}{P_y} + \frac{0.85\ M}{M_p} \leq 1.0 \qquad (5\text{-}1)$$

and restricts the bending moment at the segment ends in order to prevent local failures. The P_f term corresponds to the test axial load.

The second equation is given by:

$$\frac{P_f}{1.67P'} + \frac{C_m M\beta}{M_p} \leq 1.0 \qquad (5\text{-}2)$$

and restricts the force and moment on the segment to values less than those required to produce overall failure by excessive bending. The $1.67\,P'$ and β terms are calculated using the KL/r of the total subassemblage.

The maximum values of the lateral loads obtained during testing and those predicted using the interaction equations are listed in TABLES 5.2 and 5.3. In all cases Equation 5.2 (stability) exceeded, but was close to, unity. This indicates that the modified interaction equations predict the ultimate load carrying capacity of a beam-column subjected to a concentrated lateral load conservatively and accurately, for this series of tests. APPENDIX B contains a similar comparison for the small scale tests performed by Wright (21, 22).

Test	Point of Load Application	R_{max}	
		Test (kips)	Predicted (kips)
BC-1*	Mid-height	7.4	8.1
BC-2	Mid-height	11.1	10.4
BC-3	Mid-height	5.0	5.6
BC-4	Mid-height	18.4	17.4
BC-5	Mid-height	7.8	7.9
BC-6	Upper third-point	12.9	12.8
BC-7	Upper third-point	6.6	7.2
BC-8	Upper third-point	20.8	19.1
BC-9	Upper third-point	15.3	13.5

Note: * Tested with no restraining beams.

TABLE 5.1 EXPERIMENTAL RESULTS

Test	R_{max} Test (kips)	Maximum Segment Moment (ft-kips)	Axial Load	$\frac{P_f}{P_y}$	$\frac{.85M}{M_p}$	$\frac{P_f}{P_y} + \frac{.85M}{M_p}$ Equation 5.1
BC-1	7.4	26.2	64	0.26	0.52	0.78
BC-2	11.1	27.7	63	0.26	0.55	0.81
BC-3	5.0	12.5	110	0.45	0.25	0.70
BC-4	18.4	32.6	73	0.30	0.64	0.94
BC-5	7.8	13.8	130	0.53	0.27	0.80
BC-6	12.9	28.6	64	0.26	0.57	0.93
BC-7	6.6	14.7	111	0.46	0.29	0.75
BC-8	20.8	32.7	73	0.30	0.65	0.95
BC-9	15.3	31.6	73	0.30	0.62	0.92

TABLE 5.2 INTERACTION EQUATION (STRENGTH)

Test	G_u	G_l	K	$1.67P'$ (kips)	P_e (kips)	β	$\frac{P_f}{1.67P'}$	$\frac{C_m M\beta}{M_p}$	$\frac{P_f}{1.67P'} + \frac{C_m M\beta}{M_p}$ Equation 5.2
BC-1	∞	∞	1.00	171	226	1.39	0.37	0.72	1.09
BC-2	0.33	0.47	0.66	177	259	1.30	0.35	0.71	1.06
BC-3	0.33	0.47	0.66	177	259	1.74	0.62	0.43	1.05
BC-4	0.47	0.66	0.69	202	473	1.18	0.36	0.76	1.12
BC-5	0.47	0.66	0.69	202	473	1.38	0.64	0.38	1.02
BC-6	0.33	0.47	0.66	177	259	1.33	0.36	0.75	1.11
BC-7	0.33	0.47	0.66	177	259	1.75	0.62	0.51	1.13
BC-8	0.47	0.66	0.69	202	473	1.18	0.36	0.76	1.12
BC-9	1.41	0.66	0.76	196	410	1.22	0.36	0.76	1.12

TABLE 5.3 INTERACTION EQUATION (STABILITY)

CHAPTER VI

SUMMARY AND CONCLUSIONS

This investigation was undertaken primarily to obtain experimental results on large scale beam-columns subjected to concentrated lateral loads. In addition, an attempt was made to correlate the maximum load carrying capacities of the beam-columns with those predicted by existing analytical procedures and thus provide the basis for a design method.

The experimental program consisted of a series of nine laterally loaded beam-column subassemblages in different arrangements. The specimens were subjected to concentrated loads at either the column mid-height or upper thrid-point. All tests were continued well into the unloading range.

The experimental results obtained agreed with predictions based on a second-order elastic-plastic solution which considered the actual hinge location and the effect of strain hardening. The ratios of observed to predicted maximum loads range from 0.91 to 1.12 with a mean value of 1.01.

Finally a comparison between the maximum loads for these tests (and those obtained by Wright on small scale specimens) and those calculated from the interaction equations, showed that the interaction equations are conservative. The ratios of the load obtained experimentally to that predicted varied from 1.02 to 1.13 with a mean value of 1.09. From these results, the technique proposed and incorporated into the present Canadian specifications, appears to provide a rational method for designing laterally loaded beam-columns.

LIST OF REFERENCES

1. Adams, P.F., Lay, M.G. and Galambos, T.V., "Experiments on High Strength Steel Members," Welding Research Council Bulletin No. 110, November, 1965, pp. 1-16.

2. Adams, P.F., "Discussion of Ultimate Strength of Laterally Loaded Columns," Journal of the Structural Division, American Society of Civil Engineers, Vol. 95, ST3, March, 1969, pp. 512-516.

3. Adams, P.F., "Segmental Design of Steel Beam-Columns," Proceedings, Canadian Structural Engineering Conference, Toronto, February, 1970.

4. Adams, P.F. and McLellan, E.R., "Design of Steel Crane Columns or Columns Subjected to Lateral Loads," Transactions, Engineering Institute of Canada, EIC-70-BR & STR 9, Vol. 13, No. A-6, July, 1970, pp. I-X.

5. Arnold, P., Adams, P.F., and Lu, L.W., "Experimental and Analytical Behavior of a Hybrid Frame," Transactions, American Society of Civil Engineers, Vol. 135, No. 1, 1970, pp. 416-418.

6. CSA G40.12-1964-General Purpose Structural Steel, Canadian Standards Association, Rexdale, Ontario, 1964.

7. CSA Standard S16-1969-Steel Structures for Buildings, Canadian Standards Association, Rexdale, Ontario, 1969.

8. Commentary on CSA S16-1969, Canadian Institute of Steel Construction, Toronto, 1970.

9. Johnson, B.G., ed., Guide to Design Criteria for Metal Compression Members, Column Research Council, 2nd edition, John Wiley and Sons, New York, 1966.

10. Ketter, R.L. and Galambos, T.V., "Columns Under Combined Bending and Thrust," Transactions, American Society of Civil Engineers, Vol. 126, No. 1, 1961, pp. 1-25.

11. Ketter, R.L., "Further Studies on the Strength of Beam-Columns," Journal of the Structural Division, American Society of Civil Engineers, Vol. 87, ST6, August, 1961, pp. 135-152.

12. Lay, M.G., The Mechanics of Column Deflection Curves, Fritz Laboratory Report No. 278.12, Lehigh University, 1965.

13. Lay, M.G., Aglietti, R.A. and Galambos, T.V., "Testing Techniques for Restrained Beam-Columns," Proceedings, Second SESE Interantional Congress on Experimental Mechanics, Washington, D.C., September, 1965.

14. Lay, M.G., and Galambos, T.V., "The Experimental Behavior of Restrained Columns," Welding Research Council Bulletin No. 110, November, 1965, pp. 17-37.

15. Lay, M.G., "Flange Local Buckling in Wide-Flange Shapes," Journal of the Structural Division, American Society of Civil Engineers, Vol. 91, ST6, December, 1965, pp. 95-116.

16. Lecture Notes on the Plastic Design of Multi-Story Frames, Fritz Laboratory Report, No. 273.20, Lehigh University, 1965.

17. Lu., L.W. and Kamalvand, H., "Ultimate Strength of Laterally Loaded Columns," Journal of the Structural Division, American Society of Civil Engineers, Vol. 94, ST6, June, 1968, pp. 1505-1524.

18. Paris, C.P., "Testing of Columns with Uniformly Distributed Transverse Loads," Journal of the Engineering Institute of Canada, Vol. 37, August, 1954, pp. 945-949.

19. Tall, L., et al, Structural Steel Design, 1st edition, The Ronald Press Co., New York, 1964.

20. Timoshenko, S.P. and Gere, J.M., Theory of Elastic Stability, 2nd edition, McGraw-Hill Book Co., New York, 1961.

21. Wright, D.T., "Flexural Members and Connections Under Combined Loading," thesis presented to the University of Cambridge, at London in 1955, in partial fulfillment of the requirements for the degree of Doctor of Philosophy.

22. Wright, D.T., "The Design of Compression Beams," Journal of the Engineering Institute of Canada, Vol. 39, February, 1956, pp. 139-141.

23. Yarimci, E., Yuka, J.A. and Lu, L.W., "Techniques for Testing Structures Permitted to Sway," Experimental Mechanics, Vol. 7, No. 8, August, 1967, pp. 321-331

24. Yuka, J.A. and Galambos, T.V., "Strength of Single Story Frames," Journal of the Structural Division, American Society of Civil Engineers, Vol. 91, ST5, October, 1965, pp. 81-96.

APPENDIX A

DESIGN OF BEAM-COLUMNS

To design a beam-column for uniaxial bending, a cross-section is first assumed and the member is then checked for adequacy against two interaction equations (7). These equations relate the forces and end moments acting on the member to limiting values of the same quantities.

The first equation restricts the bending moment at the member ends in order to prevent local failures. The end moment is limited to M_{pc}, the reduced plastic moment capacity of the column in the presence of an axial load. The ultimate strength form of this equation is given by :

$$\frac{P_f}{P_y} + \frac{0.85\ M}{M_p} \leq 1.0 \qquad \text{(A.1)}$$

where P_f is the factored axial load acting on the member, M is the factored moment and M_p is the plastic moment capacity of the section.

The second equation restricts the force and end moment on the member to values less than those required to produce overall failure by excessive bending. The ultimate strength form of this equation is given by :

$$\frac{P_f}{1.67\ P'} + \frac{C_m M \beta}{M_p} \leq 1.0 \qquad \text{(A.2)}$$

where $1.67\ P'$ is the axial load permitted if axial force alone existed. The term β is equal to $1/(1 - P/P_e)$ and is the amplification factor, which attempts to account for the secondary moments produced by the axial load acting on the deformed member (20). The actual boundary conditions at the member ends are considered by adjusting the effective length of the members (9). The intent of the equivalent bending moment term, C_m, is to provide an adjustment factor in those cases where the primary bending moment is not uniform over the member length (7). If the primary bending moment is not uniform, the strength of the column will be increased since the curvature will be reduced in the regions of low moment. To account for this strength increase, the equivalent moment factor, C_m is computed as the greater of :

$$C_m = 0.6 + 0.4 \frac{M_1}{M_2} \qquad \text{(A.3 a)}$$

$$C_m = 0.4 \qquad \text{(A.3 b)}$$

where M_2 and M_1 are the larger and smaller moments respectively acting at the ends of the member. M_1 and M_2 are both positive if the member is deformed into single curvature. Equation A.3 only applies if the member ends are not allowed to translate. If translation is permitted, Equation A.3 is replaced by (24):

$$C_m = 0.85 \qquad \text{(A.4)}$$

Allowable stress forms of these interaction equations are also available (7).

APPENDIX B

SMALL SCALE EXPERIMENTS

Introduction

In this Appendix, the results of tests performed by Wright on small scale members will be summarized (21). The results of tests on rectangular and wide-flange members, subjected to various loading and restraint conditions were reported; only the tests of wide-flange shapes, particularly those subjected to a concentrated load are of interest in this report. The axial load was applied to the member initially and held constant as the deflection of the beam-column was gradually increased. All specimens were deformed well into the inelastic range.

Testing Program

Tests were performed on two different wide-flange cross-sections (series III and IV); the cross-section dimensions and average values of the properties are given in FIG. B.1. The specimens were fabricated from plates; the flanges were slotted to receive the web, and the plates were then joined by brazing. All columns tested were twenty-five inches long.

FIG. B.2 shows the loading and support conditions for the tests of interest. Specimens III-5 and III-6 were fixed-ended and subjected to central concentrated loads. The remaining specimens were either pin-ended or fixed and subjected to four equal concentrated loads to simulate uniform loading. The test program is summarized

in TABLE B.1. Several beam tests were also reported in reference 25; from the results of these tests the yield stress for the specimens considered have been estimated. Also listed in TABLE B.1 are the ultimate loads observed in each test. These values were determined from the reported load-deflection curves (21). In the three tests marked with asterisks, the specimens exhibited significant lateral deformations; the lateral bracing details were not discussed in reference 25.

Comparison of Experimental Results and Interaction Equations

The maximum lateral load capacities obtained experimentally were compared with the capacities predicted by the modified interaction equations. The application of these equations is described in detail in CHAPTER V. For members subjected to uniformly distributed loads, a C_m factor equal to 1.0 is used whereas $C_m = 0.85$ is used for a member subjected to a concentrated load (7). The comparisons are shown in TABLES B.2 and B.3. In all cases, Equation 5.2 (stability) governed. The values of this interaction equation (corresponding to the maximum lateral loads) are 0.99 and 1.00 for members subjected to concentrated loads and range from 0.98 to 1.09 for members subjected to uniform loads. It would appear that lateral buckling of specimens III-3, IV-3 and IV-6 occurred as the maximum capacity was approached and did not significantly affect the load carrying capacities.

Test	Support Condition	Loading Condition	Test Maximum R or W (kips)
III-5	Fixed	Concentrated	2.20
III-6	Fixed	Concentrated	1.90
III-2	Pinned	Uniform	1.61
III-3	Pinned	Uniform	1.26
IV-2	Pinned	Uniform	0.43
IV-3	Pinned	Uniform	0.31
IV-5	Fixed	Uniform	0.89
IV-6	Fixed	Uniform	0.80

TABLE B.1 RESULTS OF SMALL SCALE TESTS

Test	Maximum Segment Moment (in kips)	Axial Stress (ksi)	$\frac{P_f}{P_y}$	$\frac{.85M}{M_p}$	$\frac{P_f}{P_y} + \frac{.85M}{M_p}$ Equation 5.1
III-5	6.60	4.48	0.12	0.86	0.98
III-6	5.70	8.96	0.24	0.74	0.98
III-2	6.04	4.48	0.12	0.79	0.91
III-3*	4.72	8.96	0.24	0.62	0.86
IV-2	1.62	4.48	0.12	0.73	0.85
IV-3*	1.17	8.96	0.24	0.53	0.77
IV-5	1.57	4.48	0.12	0.71	0.83
IV-6*	1.41	8.96	0.24	0.63	0.87

Note: * Lateral Buckling Reported

TABLE B.2 INTERACTION EQUATION (STRENGTH)

Test	K	$\frac{1.67P'}{A}$ (ksi)	C_m	β	$\frac{P_f}{1.67P'}$	$\frac{C_m M\beta}{M_p}$	$\frac{P_f}{1.67P'} + \frac{C_m M\beta}{M_p}$ Equation 5.2
III-5	0.5	37.0	0.85	1.01	0.12	0.87	0.99
III-6	0.5	37.0	0.85	1.02	0.24	0.76	1.00
III-2	1.0	33.3	1.00	1.02	0.13	0.95	1.08
III-3*	1.0	33.3	1.00	1.05	0.27	0.76	1.03
IV-2	1.0	27.4	1.00	1.09	0.16	0.93	1.09
IV-3*	1.0	27.4	1.00	1.22	0.33	0.76	1.09
IV-5	0.5	34.0	1.00	1.02	0.13	0.85	0.98
IV-6*	0.5	34.0	1.00	1.05	0.26	0.78	1.04

Note: * Lateral Buckling Reported

TABLE B.3 INTERACTION EQUATION (STABILITY)

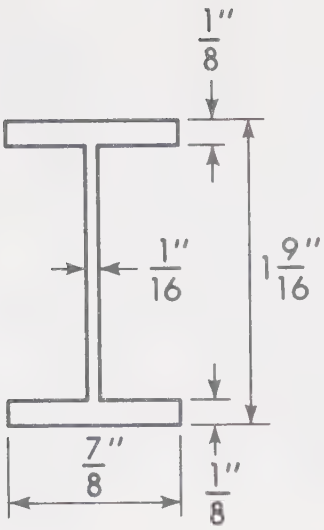

SERIES III

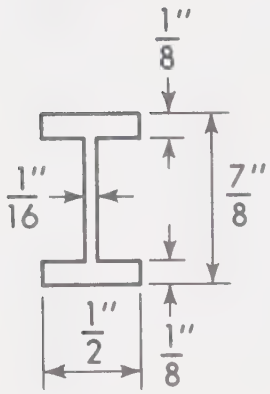

SERIES IV

FIG. B.1 CROSS-SECTION DIMENSIONS

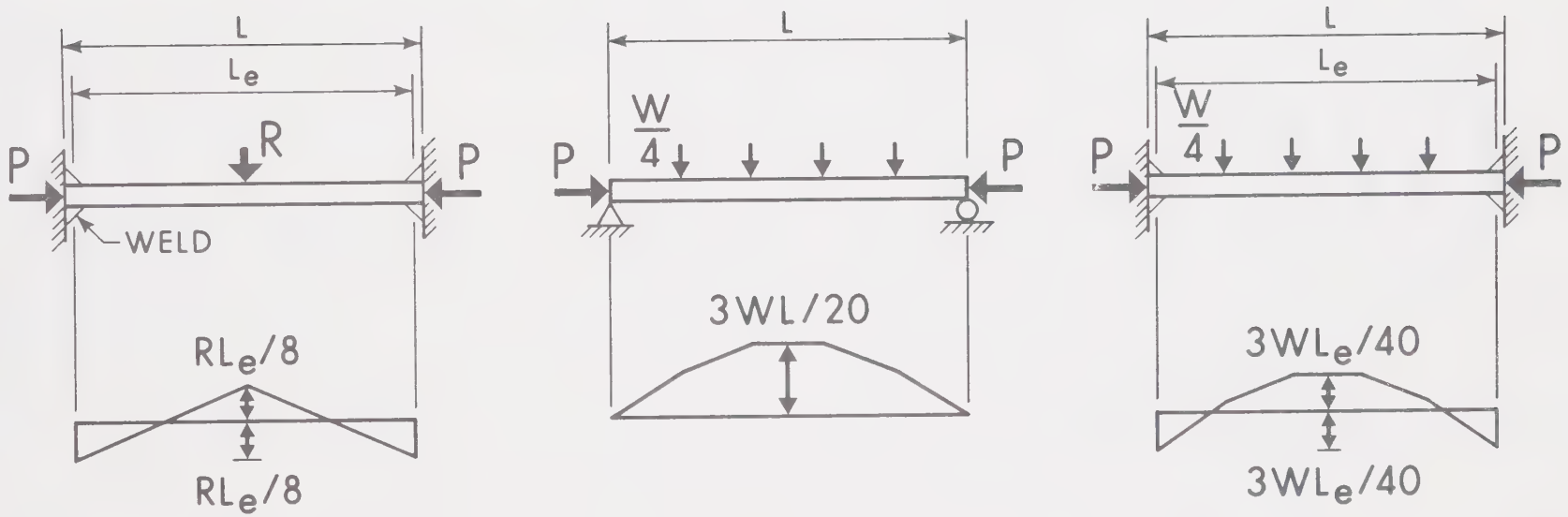

FIG. B.2 LOADING AND SUPPORT CONDITIONS

APPENDIX C

RESTRAINED COLUMN TESTS

Lay, Agliette and Galambos have proposed a novel testing arrangement for the study of the behavior of steel structures containing critically loaded beam-columns (13). The behavior of a column in a structure, such as member EB, shown in FIG. C.1, is dependent primarily on the action of the members shown within the dotted lines. Since the largest moment a beam can transmit is its fully plastic moment capacity, this group of members can be reduced to the form shown in FIG. C.2. For simplicity in testing it can be assumed that the restraints at the far ends of the beams (C and D) and the columns above E and below B, can be removed. Also since applying moments to one side of a column is more convenient, the arrangement is reoriented to the subassemblage shown in FIG. C.3. At each stage of loading the moment applied to the joint must equal the total resisting moment provided by the beam and the column. It is assumed that compatibility is enforced at the joint so that the beam and column rotations are equal. By selecting beams of varying stiffnesses it is possible to investigate the effect of the yielding sequence on the strength of the strucure. Thus it is possible to investigate the behavior of columns and beams under conditions approaching those found in real structures. Lay and Galambos used this method to test seven restrained columns bent in single curvature (14). The major advantage of this method is the ease of testing columns subjected to various loading conditions and various degrees of restraint.

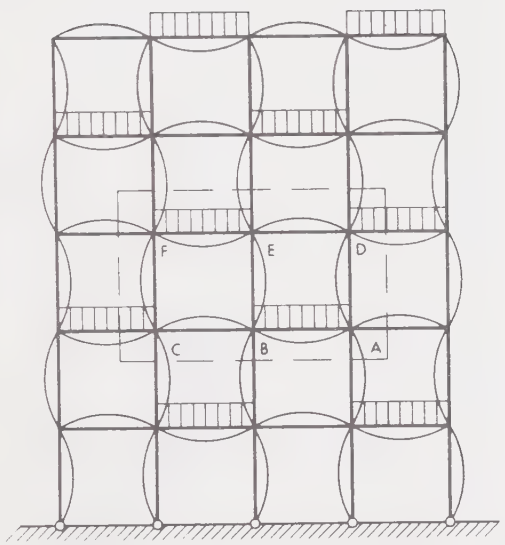

FIG. C.1 FRAME CONDITIONS

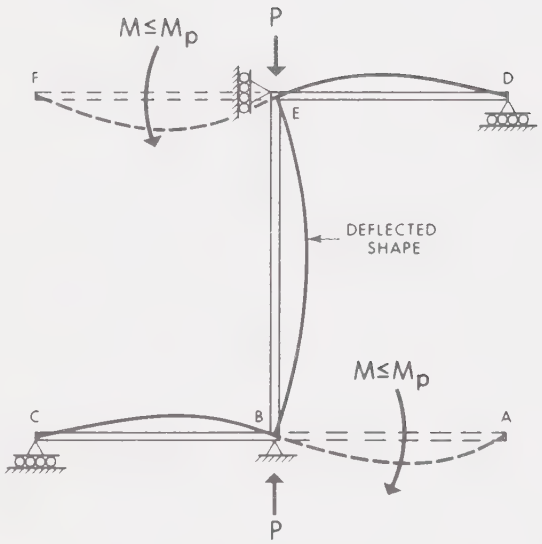

FIG. C.2 SUBASSEMBLAGE

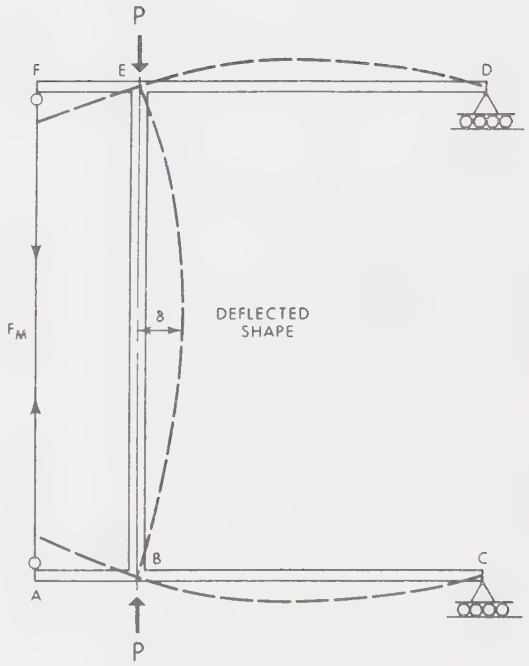

FIG. C.3 TEST SUBASSEMBLAGE

APPENDIX D

THEORETICAL PREDICTION

In order to predict the response of the subassemblage to the applied loads a program was developed to perform a second-order elastic-plastic analysis. In this procedure the position of the actual plastic hinging region was considered as well as the influence of strain-hardening (5).

In a second-order elastic-plastic analysis the response of each member (M-θ relationship) is assumed to be elastic-perfectly plastic. A second-order elastic analysis is performed until the plastic moment capacity is reached at one location in the structure. A hinge is inserted in the structure at this stage and a second-order elastic analysis is performed on the deteriorated structure under the additional loads. This procedure is repeated until a sufficient number of hinges have formed to produce a mechanism. Beyond this stage the load-deflection relationship coincides with that predicted by a second-order rigid plastic analysis. The second-order elastic-plastic analysis was formulated using the slope-deflection equations which account for the change in member stiffnesses due to axial loads. As each plastic hinge formed, the equations were modified to account for the deterioration in the structure.

The above analysis assumes that hinges form at the centers of the joints. Because of the increased strength in the area of the

connection, the hinge will form in the weaker member a distance "d" away from the face of the connection (14). To account for this, the plastic moment capacities at the centerline of each connection were increased artificially. FIG. D.1 shows the solutions, first assuming that plastic hinges occur at the centerlines of the connections and then accounting for the actual hinge locations.

The effect of strain-hardening is to increase the moment capacity above the plastic value once a hinge has formed in the structure. The influence of strain-hardening can be illustrated by considering the behavior of the cantilever beam shown in FIG. D.2 (a). The concentrated load, Q, is greater than that corresponding to a support moment of M_p. The bending moment diagram is shown in FIG. D.2 (b), where τL represents the yielded length (the length over which the moment exceeds M_p). FIG. D.2 (c) shows the (approximate) corresponding curvature distribution in the beam, and a further approximation is shown in FIG. D.2 (d). With this curvature distribution, the inelastic hinge rotation is equal to the inelastic area under the curvature diagram over the yielded length and is given by $s\ \phi_p \tau L$. Thus if the hinge rotation is known, the yielded length, support moment and load can be determined for the member. This approach was used to account for strain-hardening in the predicted subassemblage response. The inelastic hinge rotations from the second-order elastic-plastic solution were computed and the moment capacities at the hinge locations were increased as shown in FIG. D.2 (b). The yielded length, τL, was limited to l_{opt}, the optimum yielded length for local

buckling (15). The effect of strain-hardening is shown in FIG. D.1.

The actual moment-rotation (M-θ) relationship for a column segment is non-linear, due primarily to premature yielding caused by the combination of residual strains and applied loads, and under some extreme conditions the maximum moment capacity will be below M_{pc} due to the influence of instability. For the conditions particular to this series of tests, no reduction in the ultimate strengths of the column segments was anticipated (16). In addition, it has been shown previously that for the axial loads and member slendernesses involved,the neglect of the non-linearity of the M-θ relationship is not significant (5).

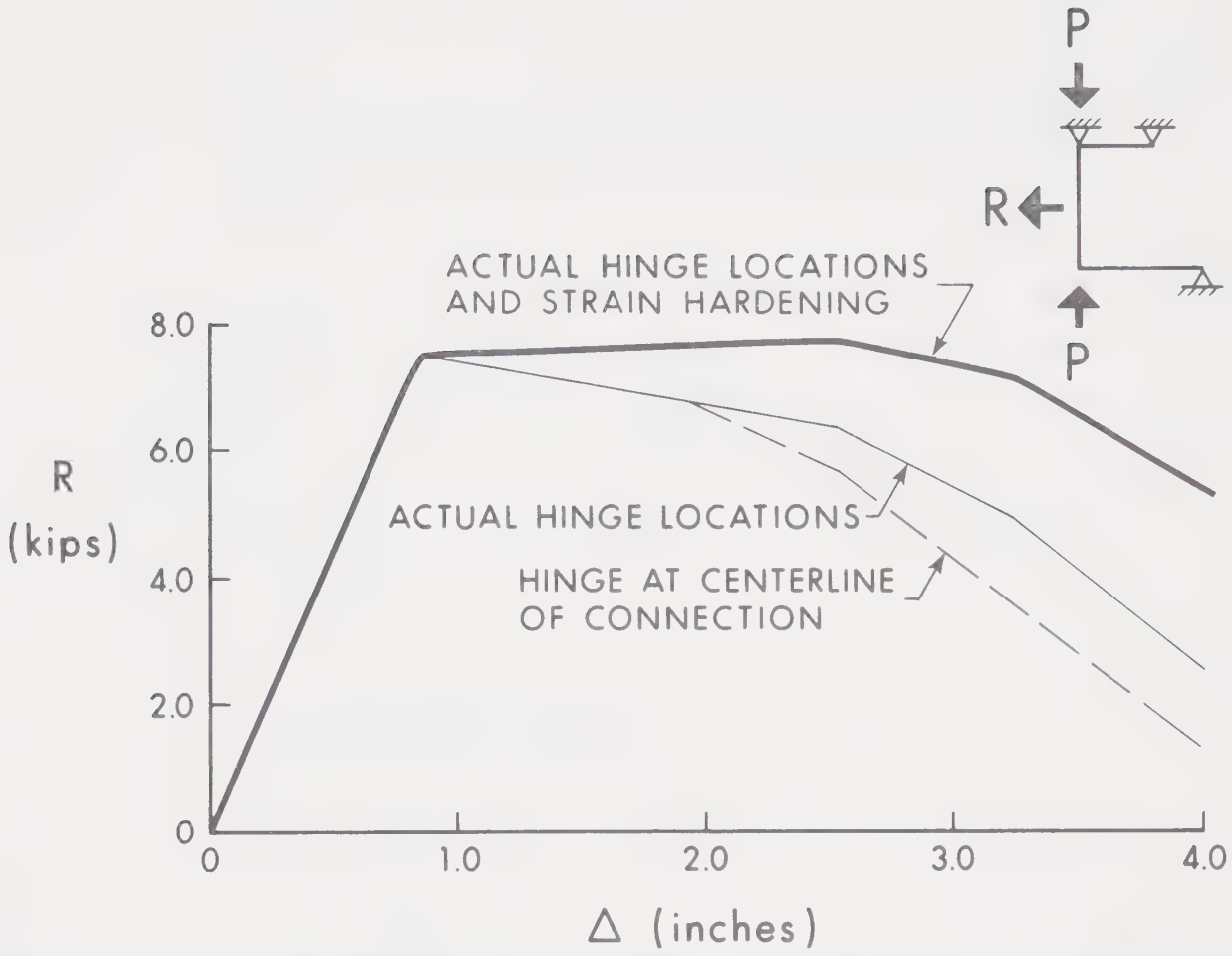

FIG. D.1 EFFECT OF HINGE SHIFT AND STRAIN-HARDENING - BC-5

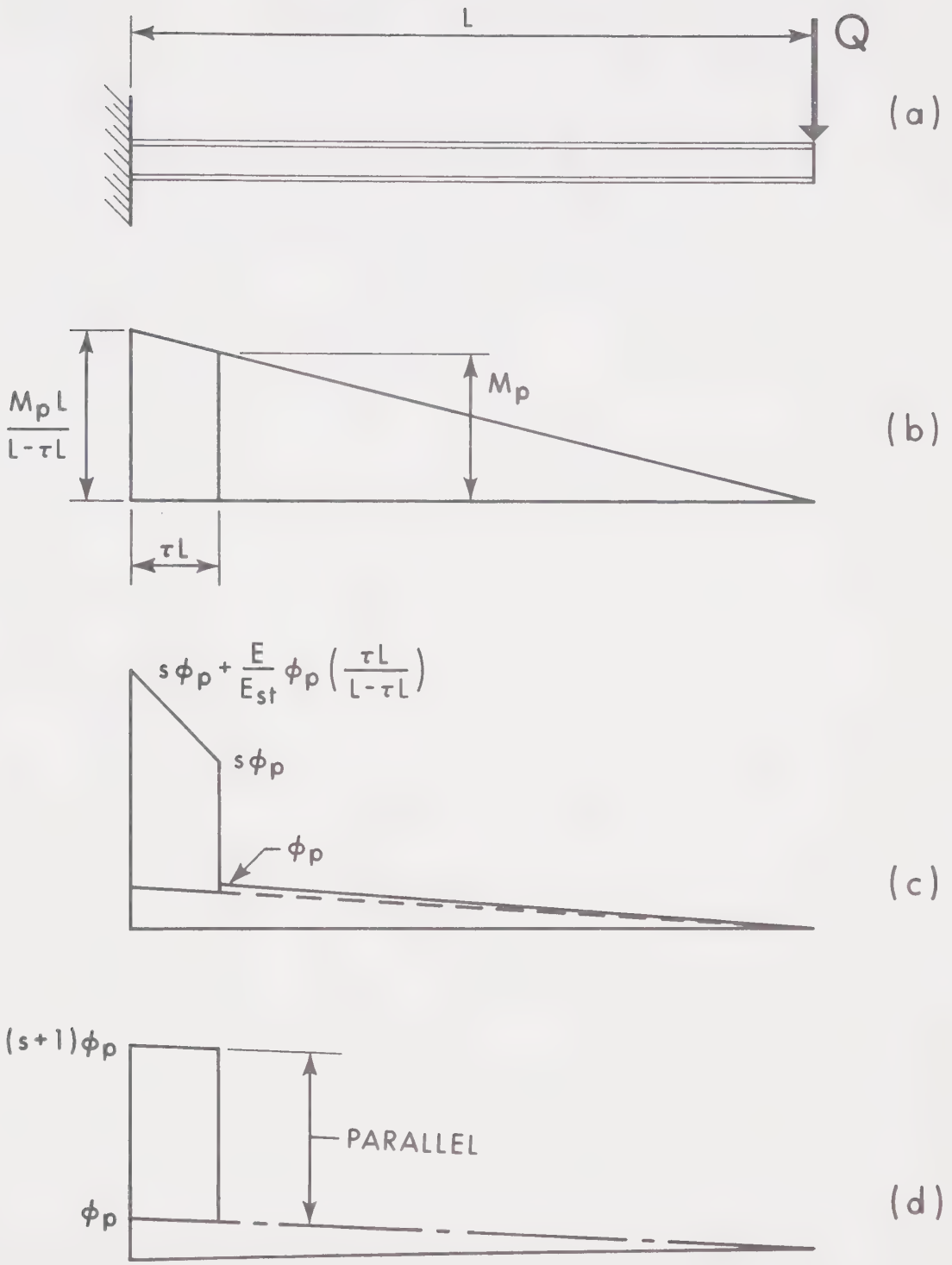

FIG. D.2 EQUIVALENT CANTILEVER